Title
A re-assessment of long distance growth and connectivity of neural stem cells after severe spinal cord injury

Authors
Sharp, Kelli G
Yee, Kelly Matsudaira
Steward, Oswald

Publication Date
2014-07-01

DOI
10.1016/j.expneurol.2014.04.008

Peer reviewed

Published in final edited form as:
Exp Neurol. 2014 July ; 257: 186–204. doi:10.1016/j.expneurol.2014.04.008.

A re-assessment of long distance growth and connectivity of neural stem cells after severe spinal cord injury

Kelli G. Sharp[a], **Kelly Matsudaira Yee**[a], and **Oswald Steward**[a,b,*]

[a]Reeve-Irvine Research Center, University of California at Irvine School of Medicine, Irvine, CA 92697, USA

[b]Departments of Anatomy & Neurobiology, Neurobiology & Behavior, and Neurosurgery, University of California at Irvine School of Medicine, Irvine, CA 92697, USA

Abstract

As part of the NIH "Facilities of Research Excellence—Spinal Cord Injury" project to support independent replication, we repeated key parts of a study reporting robust engraftment of neural stem cells (NSCs) treated with growth factors after complete spinal cord transection in rats. Rats (n = 20) received complete transections at thoracic level 3 (T3) and 2 weeks later received NSC transplants in a fibrin matrix with a growth factor cocktail using 2 different transplantation methods (with and without removal of scar tissue). Control rats (n = 9) received transections only. Hindlimb locomotor function was assessed with the BBB scale. Nine weeks post injury, reticulospinal tract axons were traced in 6 rats by injecting BDA into the reticular formation. Transplants grew to fill the lesion cavity in most rats although grafts made with scar tissue removal had large central cavities. Grafts blended extensively with host tissue obliterating the astroglial boundary at the cut ends, but in most cases there was a well-defined partition within the graft that separated rostral and caudal parts of the graft. In some cases, the partition contained non-neuronal scar tissue. There was extensive outgrowth of GFP labeled axons from the graft, but there was minimal ingrowth of host axons into the graft revealed by tract tracing and immunocytochemistry for 5HT. There were no statistically significant differences between transplant and control groups in the degree of locomotor recovery. Our results confirm the previous report that NSC transplants can fill lesion cavities and robustly extend axons, but reveal that most grafts do not create a continuous bridge of neural tissue between rostral and caudal segments.

Keywords

Spinal cord injury; Rat; BBB scale; Fibrin; Thrombin; Axonal growth; Axon regeneration; Reticulospinal tract; 5HT; Serotonin; Sprouting; Motor system; Recovery of function

[*]Corresponding author at: Reeve-Irvine Research Center, University of California, Irvine, 1105 Gillespie Neuroscience Research Facility, Irvine, CA 92697-4265, USA. Fax: +1 949 824 2625. osteward@uci.edu (O. Steward).

Introduction

In recent years, there have been numerous reports of interventions that enhance sparing of function and/or promote repair mechanisms including axon regeneration so as to enhance recovery of function after spinal cord injury. A barrier to translation is that there are often no published replications of promising studies, raising questions about reproducibility. To address this, the National Institute of Neurological Disorders and Stroke (NINDS) launched the "Facilities of Research Excellence—Spinal Cord Injury" (FORE-SCI) replication project, in which promising published studies are independently replicated. Studies are selected for replication by an independent scientific advisory committee and executed by one of the sites funded by the FORE-SCI Project. Here, we repeat an experiment that reported remarkable outgrowth of axons from transplants of neural stem cells (NSCs) that were treated with a cocktail of growth factors and transplanted into the lesion site after complete transection of the spinal cord (Lu et al., 2012).

The study of Lu et al. was based on previous evidence that regeneration failure after CNS injury was due to a combination of factors including myelin-derived inhibitors (Buchli and Schwab, 2005; He and Koprivica, 2004), inhibitory molecules expressed by reactive astrocytes near the injury site (Busch and Silver, 2007; Fitch and Silver, 2008), and lack of intrinsic growth capacity (Jones et al., 2001), for a recent review, see (Tuszynski and Steward, 2012). Previous work demonstrating axon regeneration through peripheral nerve grafts in the CNS documents that adult neurons can regenerate their axons to some extent when provided with an optimal tissue environment (David and Aguayo, 1981; Houle et al., 2006), but growth is limited due to neuron-intrinsic mechanisms (Filbin, 2006; Liu et al., 2010). The study of Lu et al. was based on the commonly held belief that a combinational treatment would be most effective. The specific approach was to transplant freshly dissociated neural stem cells/progenitors from rat embryos as in previous studies (Lepore and Fischer, 2005), but pre-treating cells with a growth factor cocktail and transplanting with a fibrin matrix. The injury model was a complete transection at thoracic level 3 (T3). Complete spinal cord transections are considered the most stringent test of regenerative strategies (Tuszynski and Steward, 2012).

We repeated key experiments in the original study to assess reproducibility, focusing on the portion of the report that used freshly isolated NSCs from fetal rats. Our results confirm that NSC transplants engraft and differentiate, although the extent of engraftment was variable and depended on the method of transplant. Our results also confirm remarkable axon outgrowth from NSC transplants. There was only limited ingrowth of host axons, however. Assessments of locomotor function did not reveal statistically significant differences between transplanted and control groups. A completely unexpected finding was that in about 50% of the rats, ectopic masses of graft-derived cells were found at long distances from the transplant site including in the brain. We report the existence of these ectopic colonies separately (Steward et al., 2014). Our findings identify important issues relating to the potential use of NSC transplants for therapy for severe SCI, including a need to further refine transplantation techniques.

Materials and methods

Details regarding the way that the FORE-SCI Replication contracts operate are summarized in perfect Steward et al., 2012. In brief, an independent Scientific Advisory Committee for the contract reviews the literature and selects papers for replication. Selection factors include: 1) Clinically-relevant endpoints (usually recovery of function); 2) Trans-latability; 3) Effect size; and 4) Scientific quality of the target paper. The Committee may select only part of the published study for replication (a particular set of experiments), and may recommend additional control groups or analyses. Experiments that were not part of the original paper, including additional control groups, are not supported by the Contract unless recommended by the Scientific Advisory Committee. Here, the Committee selected the portion of Lu et al. (2012) involving transplants of rat NSCs, with assessment of engraftment, axon outgrowth from the graft, ingrowth of host axons, and assessment of locomotor function.

Experimental animals were female Fischer 344 rats from Harlan Labs that were 10–11 weeks old at the start of the experiments (the same strain, sex, and age used by Lu et al.). Experimental protocols on spinal cord injured rats were approved by the Institutional Animal Care and Use Committee (IACUC) at the University of California, Irvine. Rats genetically engineered to express EGFP (F344-Tg(UBC-EGFP)F455Rrrc) were obtained from the Rat Resource & Research Center (P40D011062) and were bred locally to obtain embryos in the animal facilities at the Veteran's Hospital San Diego. Procedures used to collect fetal NSCs were approved by the IACUC at the Veteran's Hospital San Diego.

Every effort was made to duplicate procedures used by Lu et al. In this regard, Dr. Lu consulted on the procedures and trained our surgical staff. Because this is a surgical intervention, and as such may depend on skills that can only be mastered by extensive experience, we felt that the goals of the replication would be best-served if the same surgeon actually performed the transplants. Accordingly, Dr. Lu traveled to UCI to perform the surgical procedures with the aid of our staff. Also, to insure comparability of NSC transplants, the cells were harvested and prepared in Dr. Lu's lab at the Veterans Administration Medical Center, San Diego (VAMC) and were delivered to UCI on the day of the grafting procedure. We felt that this would be consistent with the goals of the replication because the cells could be considered to be a “product” that was obtained for use as a therapeutic agent in much the same way as a drug from a commercial entity.

Overall experimental plan and group formulation

In the original study, transplantation surgeries were performed on 5–6 rats a day generating a total of 55 rats with full transection injuries. There was no description in the original publication of how surgeries were distributed over time, how rats were assigned to groups and whether group assignment was random.

In our replication, rats were randomly assigned to 2 groups at the time of the transection surgery. A study member who was not involved in the behavioral assessment used a random generator to determine the order of surgery and the group assignments. A)one group was designated to receive transections only. B) one group was designated to receive transections

and then grafts 2 weeks later. It is important to note that although the control group (A) did not receive any treatment at the time rats in Group B received grafts, they were anesthetized and received a skin incision that was closed with staples so that the experimenters could remain blind as to group identity. Six rats that received transections and grafts received BDA injections into the reticular formation; grafted animals were randomly chosen from each squad using a random number generator. Rats that received transections and grafts and exhibited recovery of locomotor function received a secondary full transection rostral to the original graft site 6 weeks post-transplant. The schedule of surgeries is summarized in Table 1.

For Squad 1 (n = 6) the transection surgery sequence by treatment group was B, B, B, B, A, B. The same group's sequence for transplantation was B, B, A,B, B and B. Four of the six rats received grafts with removal of scar tissue (Method 1, see below); one rat received 9-point injections without scar removal (Method 2).

For Squad 2 (n = 6) the transection surgery sequence by treatment group was A,B, B, B,B, B the same group's transplantation sequence was B, B, B, B, B and A. Grafts were done with scar removal (Method 1).

For Squad 3 (n = 9) the transection surgery sequence by treatment group was A, B, A, B, A, A, B, B, B and the group's transplantation sequence was B, A, B, A, A, B, B, B, A. Grafts were done using the 9-point injections without scar removal (Method 2).

For Squad 4 (n = 8) the transection sequence by treatment group was B, A, B, B, A, A, B, B and the group's transplantation sequence was B, A, B, A, B, B, B, A. Grafts were done using the 9-point injections without scar removal (Method 2).

Spinal cord injury

Rats were anesthetized with ketamine (67 mg/kg) and xylazine, (0.7 mg/kg) and placed on a platform to eliminate movement. Respiratory pattern was monitored throughout the entire duration of the surgery. A laminectomy was performed at thoracic level 3 (T3) and a longitudinal 2 mm cut was made in the dura mater with a #11 blade. Using irridectomy scissors (Roboz, Gaithersburg, MD: cat # RS-5619), a 1.0–1.5 mm longitudinal block of spinal cord was cut on the right side and removed by aspiration with a 23 G blunt needle leaving a 1.0–1.5 mm gap. The same procedures were performed on the left completing the full transection and the site was visually inspected under a dissecting microscope to ensure that the transection was complete ventrally and laterally. Care was taken to preserve the dura mater so that transplanted cells would be confined within the lesion cavity, and to spare dorsal roots. After achieving hemostasis, overlying muscles were sutured with 4–0 silk (Henry Schien, Dublin, Ohio, 100–6830) and NeoPredef antibiotic powder (Western Medical Supply, Arcadia, CA, 94030) was applied, then the skin was closed using wound clips (Fisher Scientific, Pittsburg, PA).

Animal care

Following surgery, rats were placed in cages on water circulating jacketed heating pads for the duration of the study. After recovering from the anesthetic, animals were housed 3–4 per

cage. After surgery, rats received lactated ringers (20 ml/kg, subcutaneously) every 6 h for the first 3 days and then as needed. Rats also received banamine (Butler Schein, Visalia, CA, cat #001846) (2 ml/kg, subcutaneously) every 12 h for the first 3 days and subcutaneous injections of ampicillin (Western Medical Supply, Arcadia, CA; cat #6127) 3 ml/kg every 24 h for the first 14 days or until bladder function returned. For the entire duration of the study, rats were given sulfamethoxazole and trimethoprim (Butler Schein, Visalia, CA, cat #032455) (40 mg/8 mg per 1 mL) and amoxicillin (Western Medical Supply, Arcadia, CA, #750) (50 mg/1 mL) in drinking water (1–2 ml per 80–100 ml of water). The medicated water was changed every 3 days. Bladders were expressed 2–3 times daily by manual crede until reflex bladder function returned. Rats were fed Nutri-Cal (Butler Schein, Visalia, CA; cat #000790) and DietGel (ClearH2O, Portland, ME, cat #72-06-5022) for the first two weeks. Staples were removed 14 days post grafting.

Rats were monitored 2–3 times daily for general health, coat quality (indicative of normal grooming activity) and mobility within the cage. Rats with full transection injuries typically resume these activities 3–4 days following injury. In addition, signs of paralysis were monitored, including hindlimb paralysis, tail flaccidity, instability and uncoordinated movement. Animals were also monitored for signs of skin lesions on the paralyzed limbs or autophagia of the toes (there were no skin lesions or incidents of autophagia).

Cell preparation

Timed-pregnant female rats (Strain: F344-Tg(UBC-EGFP)F455Rrrc; Rat Resource and Research Center Columbia, MO, RRRc# 00307) were deeply anesthetized with an IP injection of Euthasol (100 mg/kg). The abdominal cavity was opened under aseptic surgical conditions using scissors and the uterus was removed and placed in a Petri dish with cold PBS on ice. The dam was then sacrificed by performing a thoracotomy. A cut was made along the length of both uterine horns and embryos were removed and placed on a Petri dish with cold PBS on ice. Embryo age was verified by the presence of clear lines separating the digits of the developing forepaws. E13 digits are still fused and E13.5 are partially separated. A “NightSea” flashlight (Electron Microscopy Sciences, Hatfield, PA, DFP-1) was used to identify GFP-positive embryos. One and one half GFP-positive E14 embryos were collected for each rat to be transplanted.

For dissection, each embryo was placed in a dry Petri dish, the head and tail were removed, and the embryo was positioned in a prone position with limbs extended. Using micro-scissors a cut was made through the light transparent skin layer along the dorsal midline from neck to tail, to expose the spinal cord. The ventral lamina and underlying tissue was separated on both sides by gentle probing with fine micro-forceps (Roboz, Gaithersburg, MD, RS5010# 55). The spinal cord was removed and placed in a Petri dish with sterile saline. Under high magnification, the dura mater was removed using fine forceps and the spinal cord was rinsed several times in fresh sterile saline

Dissociation of fetal spinal cord

Spinal cords were transferred to 15 ml conical tubes containing 1 ml of ice cold HBSS (Calcium and Magnesium free) (Gibco, Grand Island, NY, cat# 14175095), and 1 ml of

0.25% Trypsin-EDTA (Gibco, Grand Island, NY; cat# 25200056) was added bringing the final volume to 2 ml and final Trypsin concentration to 0.125%. Tubes were placed in a 37 °C water bath for 8–15 min. After incubation, 10 ml of DMEM (Gibco, Grand Island, NY, 11995073) containing 10% FBS (Gibco, Grand Island, NY, 16000044) was added to stop the trypsin reaction. Tubes were centrifuged at 2500 RPM for 2 min, the supernatant was removed, and 1 ml of Neurobasal medium with 1:50 B27 growth promoting supplement (Gibco, Grand Island, NY, 17504044) was added. The pellet was gently re-suspended with a 1 ml pipet-man and large sterile pipet tip, and then a fire polished Pasteur pipet with large bore was used to triturate the cell suspension. Re-suspension was continued by triturating with progressively smaller diameter fire polished pipettes, and cells were pelleted by centrifugation at 2500 RPM for 2 min. The supernatant was removed and the pellet was re-suspended in 1–2 ml of Neurobasal medium then filtered through 45 μm cell strainer and collected into a sterile 50 ml tube. All of the above procedures were performed at VAMC and required approximately 2 h per preparation.

Immediately prior to transplantation, cells were counted on a cytometer, pelleted at 2500 RPM for 2 min, then re-suspended at a final concentration of 250,000 cells/μl in a fibrin and thrombin cocktail. The fibrin and thrombin/cocktail/cell mixture was loaded in separate glass pulled pipettes. Injection parameters are described below.

Preparation of fibrogen/thrombin/cocktail

The growth factor cocktail contained the following agents: recombinant human brain-derived neurotrophic factor (BDNF, 50 μg/ml, Peprotech, Rocky Hill, NJ; cat 452–02), recombinant human neurotrophin-3 (NT-3, 50 μg/ml, Peprotech,-03), calpain inhibitor III (MDL28170, 50 μM, Sigma Aldrich, St. Louis, MO, M6690), human platelet-derived growth factor-AA (PDGF-AA, 10 μg/ml, Sigma Aldrich, P3076), mouse insulin-like growth factor-1 (IGF-1, 10 μg/ml, Sigma Aldrich, I8779), murine epidermal growth factor (EGF, 10 μg/ml, Sigma Aldrich, E1257), basic human fibroblast growth factor (bFGF, 10 μg/ml, Sigma Aldrich, F0291), acidic human fibroblast growth factor (aFGF, 10 μg/ml, Sigma Aldrich, F5542), rat glial cell line-derived neurotrophic factor (GDNF, 10 μg/ml, Sigma Aldrich, G1401), and human he-patocyte growth factor (HGF, 10 μg/ml, Sigma Aldrich, H9661). Each original agent was reconstituted in 1×phosphate-buffered saline (PBS). Rat fibrinogen (100 mg/ml, Sigma Aldrich, F6755) and 1×PBS were combined with the growth factor cocktail and made into aliquots with a final concentration of 25 mg/ml. Rat thrombin (100 U/ml, Sigma Aldrich, T5772) and10 mM $CaCl_2$ was combined with the growth factor cocktail and made into aliquots with a final concentration of 25 U/ml. One aliquot of rat fibrinogen/growth factor cocktail (25 mg/ml) and one aliquot of rat thrombin/growth factor cocktail (25 U/ml) were used on the day of transplantation surgeries.

Grafting procedures

Two weeks post injury rats were re-anesthetized with ketamine/ xylazine as above. Rats were placed in a stereotaxic device with a tail clamp, the skin over the laminectomy site was incised, and muscle and scar tissue were dissected to expose the original laminectomy site taking care not to reinjure the dura mater and spinal cord.

In the original study, two different methods were used for grafting. This was not reported in their Methods section, but was communicated to us by the original author. The original authors felt that it was important to use both methods in our replication experiment so that there could be a direct comparison. The major difference between the two methods is that in Method 1, scar tissue was removed prior to transplant.

Method 1—The dura mater was incised and scar tissue was carefully aspirated creating a cavity without injuring the spinal cord (Fig. 1). Then 3.0 μl of the fibrogen/cocktail/cells was injected into the epicenter of the lesion using a Picospritzer (Parker, Hollis, NH,052–0500–900) and a preformed gel made out of 50 μg/ml of fibrin and 50 g/μl of thrombin was placed over the cavity. Then 0.375 μl thrombin/cocktail/cells was injected into eight sites (two sites lateral to the epicenter and three sites rostral and three sites caudal to the epicenter) (Fig. 1).

Method 2—A series of nine holes were made in the dura mater (Fig. 1) using a 1 cm^3 insulin syringe with a 30Ga needle. Three holes were rostral to the epicenter, three were at the epicenter, and 3 were caudal to the epicenter. Each hole was expanded until the ventral spinal column was identified leaving the scar tissue intact, taking care not to damage the intact spinal cord (Fig. 1). Using a Picospritzer, 1.5 μl of fibrogen/cocktail/cells was injected into the central site at epicenter, 1.0 μl was injected in the two lateral points at the epicenter and 0.33 μl was injected into each site rostral and caudal to the epicenter. Then the same procedure was repeated with the mixture of thrombin/cocktail/ cells.

Each of the transplantation methods delivered approximately 6–7 μl of fibrin/thrombin/cocktail/cells mixture into the lesion site and approximately 250,000 cells per μl for a total of approximately 1.5×10^6 cells per graft. Nine rats were injected using Method 1; eleven were injected using Method 2 (see Table 2).

After achieving hemostasis, overlying muscles were sutured and the skin was closed using wound clips as described above. Post-operative care was as described above.

Timing of procedures

NSC's were harvested in the morning at VAMC between approximately 7 and 9 AM. The cells were transported to UCI on ice, where the first transplant surgery was carried out at about 11 AM, with other rats receiving transplants at intervals of approximately 30 min. Transplants were done on 4 different days. The number of rats that received transplants on particular days and the timing of transplant delivery for individual rats is shown in Table 2.

Re-transection of the spinal cord

Nine weeks post injury two rats with transplants that exhibited locomotor recovery received a secondary full transection. For this, rats were re-anesthetized with ketamine/xylazine, the skin was incised and muscle and scar tissue were carefully dissected to expose the original laminectomy site paying special attention not to re-injure the dura mater and spinal cord. The spinal cord was transected rostral to the graft with a #11 scalpel blade, and the site was visually inspected under a dissecting microscope to ensure that the transection was complete ventrally and laterally. After achieving hemostasis, overlying muscles were sutured and the

skin was closed using wound clips as described above. Post-operative care was as described above.

BDA injections

Nine weeks post lesion, six rats received bilateral injections of biotin dextran amine (BDA) (Molecular probes, Carlsbad, CA, D1956; 10% in saline) into the reticular formation to label descending reticulospinal axons (Jin et al., 2002). These rats were randomly chosen by a random number generator. Injections were made at 4 sites, delivering 0.5 μl per site (see Table 3 for coordinates).

Functional assessments

Bladder function—Following spinal cord injury, deficits in bladder function are reflected by an inability to empty the bladder, which can be quantified by measuring the volume of urine retained in the bladder. To assess urine retention, expressed urine was collected and weighed once each week during the routine bladder expression in the morning.

Hindlimb locomotor function (BBB)—Hindlimb locomotor function was assessed with the BBB locomotor rating scale (Basso et al., 1995). BBB testing was carried out prior to injury and once weekly for seven weeks post-injury. Baseline testing occurred twice prior to injury. For testing, rats were placed in an open field (a galvanized stock tank that was 105 cm in diameter with 30 cm high walls) for 4 min. *The BBB* is a 0–22-point scale designed to assess hind limb locomotor recovery after injury to the thoracic spinal cord. This scale provides a measure of hindlimb function ranging from complete paralysis to normal locomotion by assessing hind limb joint movements, stepping, trunk position and stability, forelimb–hindlimb coordination, paw placement, toe clearance, and tail position. Rat's bladders were expressed manually 20–25 min prior to testing in the open field. BBB testing was done just after animal care in the morning, and so there was typically only a small amount of expressible urine at the time of BBB testing. Hindlimb movement and locomotion were scored simultaneously by two observers (both blind to the treatment groups) who focused on different sides of the animal.

Histological procedures

Rats were euthanized 9–10 weeks post-injury via injection of Euthasol (100 mg/kg), and were perfused transcardially with 4% paraformaldehyde in 0.1 M phosphate buffer,pH 7.4. Spinal cords and brains were removed and post-fixed in 4% paraformaldehyde in 0.1 M phosphate buffer, pH 7.4 at 4 °C overnight and were then cryo-protected in 27% sucrose.

A 15 mm block of spinal cord containing the lesion was embedded in OCT Tissue-Tek (Sakura Finetek, USA Inc., 25608–930) and frozen. Cryo-stat sections were taken in the horizontal plane at 30 μm, and sections were collected in serial order in PBS with 0.05% sodium azide. For each stain described below, every 6th section was taken to create a series that spanned the depth of each spinal cord with 180 μm between sections. Blocks of the spinal cord at spinal levels C2, C4, C6, C8, T6, T8, T10, T12, L1/2, and L4 were sectioned in the transverse plane at 20 μm.

For rats that received a BDA injection, brains were prepared as above and sectioned at 20 μm thickness in the coronal plane. Sections at 200 μm intervals were stained for BDA to document the injection sites. Transverse sections rostral and caudal to the segment of spinal cord containing the lesion were also stained for BDA to assess the distribution of BDA-labeled axons above and below the level of the injury. Brains from rats that did not receive BDA were sectioned in the coronal plane at 20 μm or 40 μm and sections at 100–120 μm intervals were immunostained for GFP.

Spinal cord sections were analyzed to assess lesion characteristics, extent of engraftment, and where BDA was involved, BDA labeling. Sets of horizontal sections from rats that did not receive grafts were stained for GFAP to define the region of activated astrocytes, and neurofilament to assess whether there were surviving axons at the injury site. One set of sections from rats with transplants was stained for GFP only to allow for quantitative assessment of GFP-positive fibers extending into the host tissue. Sets of sections were also co-stained for GFP to label the graft and GFAP to define the region of activated astrocytes, or co-stained with GFP and SMI-312 (neurofilament). Representative sections from some animals were immunostained for cell type-specific markers NeuN, APC, or Iba1 to characterize the graft composition. Sections from rats that received BDA were stained for BDA to visualize the labeled reticulospinal axons in the spinal cord.

For immunostaining, sections taken at 180 μm intervals through the lesions or cross-sections of spinal cord and brain were washed in TBS, blocked in TBS with 0.1–0.3% Triton X-100 and 5% normal donkey or goat serum, then incubated overnight in primary antibody cocktails containing as needed, rabbit anti GFP 1:1500 (Invitrogen, Carlsbad, CA, A-11122), mouse anti GFAP 1:1000 (Sigma-Aldrich, St. Louis, MO, G-3893), mouse anti SMI-312 for neurofilament 1:1000 (Abcam, Cambridge, UK, ab24574), rabbit anti-5-HT 1:1000 (Sigma-Aldrich, St. Louis, MO, S-5545), mouse anti-MAP2 1:500 (Sigma-Aldrich, St. Louis, MO, M9942), mouse anti APC 1:400 (Oncogene, LaJolla, CA, OP80-100UG), mouse anti NeuN 1:200 (Millipore, Burlington, MA, MAB377), rabbit anti Iba1 1:1000 (Wako, Osaka Japan, 019-19741). Sections were washed in TBS, and then incubated with Alexafluor conjugated secondary antibodies diluted 1:250 in TBS with 5% normal donkey or goat serum. For GFP and 5-HT, donkey anti-rabbit Alexafluor 488 (Invitrogen, Carlsbad, CA, A-21206) or Alexafluor 594, for GFAP, MAP2 APC, NeuN, and SMI312 and, donkey anti-mouse Alexafluor 594 (Invitrogen, Carlsbad, CA, A-21203), 5HT and Iba1 was used. Following washes, sections were stained in 1 μg/ml Hoescht 33258 (Molecular Probes, Eugene, OR, H-3569) for 5 min, washed in TBS, and mounted in serial order on gelatin subbed slides. Slides were coverslipped with Vectashield (Vector Laboratories, Burlingame, CA, H-1000).

For GFP immunostaining, free-floating sections were washed in TBS, treated in 1% hydrogen peroxide for 15 min, washed again in TBS, then blocked in TBS with 0.1% Triton X-100 and 5% normal donkey serum. Sections were incubated in rabbit anti-GFP 1:1500 (Invitrogen, Carlsbad, CA, A-11122) overnight, washed in TBS, then incubated with donkey ant-rabbit-HRP secondary antibody (Jackson ImmunoResearch laboratories, Inc., West Grove, PA, 711-036–152) 1:250 1–2 h. Sections were washed in TBS and reacted with nickel enhanced DAB (Vector Laboratories, Burlingame, CA, PK4100), rinsed, then

mounted on gelatin-subbed slides. Slides were dehydrated through graded ethanols, cleared in Xylenes, and coverslipped with DPX.

To co-stain for BDA and GFP, sections were washed in TBS with 0.1% Triton X-100, blocked in TBS with 5% normal donkey serum, then incubated with streptavidin-Alexafluor 594 1:250 (Invitrogen, Carlsbad, CA, S-11227) and rabbit anti-GFP 1:1500 (Invitrogen, Carlsbad, CA, A-11122) overnight. Sections were washed in TBS, and incubated with donkey anti-rabbit Alexafluor 488 (Invitrogen, Carlsbad, CA, A-21206) diluted 1:250 in TBS with 5% normal donkey serum. Sections were washed in TBS, mounted on gelatin-subbed slides, and coverslipped with Vectashield (Vector Laboratories, Burlingame, CA, H-1000). (see Table 4 for histological summary).

Quantification of GFP-labeled axons

To determine the number of GFP-positive axons extending from the graft, we assessed axons in one set of horizontal sections taken at 180 μm intervals. A line was drawn from one side to the other in each horizontal section 500 μm caudal to the graft/host interface. GFP-labeled axons crossing this line were marked and counted under 600×magnification.

Quantification of GFP-labeled axon density

Images were captured under 40×magnification 500 μm caudal to the graft/host interface. Using ImageJ software, the threshold was adjusted so that GFP-labeled axons were above threshold. The same threshold was used for each image for all the animals. Measurements were then taken in each section of the series taken at 180 μm intervals. The axon densities were summed and divided by the number of sections. Data are expressed as pixels/unit area.

Statistical evaluation

In all quantification procedures and behavioral analyses, observers were blinded to treatment groups. Multiple group comparisons were made using one-way analyses of variance. Two-group comparisons were tested by Student's *t*-test. Analyses were performed using Graph Pad Prism (La Jolla, CA).

Results

Rats received spinal cord injuries on 4 separate days over a period of two weeks (termed Squad 1–4). On each surgery day, rats were randomly assigned to grafted or lesion only control groups as described in the Methods. Table 5 summarizes the numbers for each squad, and attrition due to all causes, and removal from the study.

Attrition and final group numbers

Of the 7 rats that received T3 transections on 4/23/13, one was removed from the study because of incomplete paralysis (BBB greater than 7 at 14 days post-lesion). Five of the remaining rats received transplants, and one was a non-transplant control. One of the transplanted rats received a BDA injection, and one received a secondary re-transection. None of the rats died during or following the injury, transplantation, tract tracing or re-transection surgeries.

Of the 7 rats that received T3 transections on 4/26/13, one rat died post injury. Five rats received transplants, and one was a non-transplant control. One of the transplanted rats received a BDA injection, but died at the time of this procedure. Tissue was collected from this animal and was included in the E14 grafted group for histological and behavioral analysis. Another received a secondary re-transection, but was euthanized and perfused 2 days after the secondary lesion due to poor health. We included data from this rat in the histological and behavioral analysis.

Of the 10 rats that received T3 transections on 4/30/13, one was removed from the study because of incomplete paralysis. Of the remaining rats, 5 rats received transplants, and 4 were non-transplant controls. Two of the transplanted rats received BDA injections, and one rat died at the time of this procedure. We were able to perfuse the rat that died so data from this rat are included in the histological and behavioral analysis.

Of the 11 rats that received T3 transections on 5/2/13, three rats died 1-day post injury. Five rats received transplants, and 3 were non-transplant controls. Two of the transplanted rats received BDA injections. None of the rats died during or following transplantation or tract tracing.

In optimal cases, NSC grafts survive and expand to fill the lesion cavity

Fig. 2 illustrates examples of lesion sites in non-grafted control rats and rats that received transplants. These are horizontal sections that were immunostained for GFAP (in the case of the non-grafted controls) and co-stained for GFAP and GFP in the case of sections from rats that received transplants.

In non-grafted controls, the stumps of the spinal cord at the lesion site were capped with a glial/connective tissue scar and GFAP staining was highly elevated in the zones adjacent to the lesion margins (Fig. 2A). Non-neural scar tissue (GFAP negative) was present in the lesion site in a trabecular network, and GFAP-positive processes extended partially into the scar tissue. In none of the cases was there evidence of a spared bridge of neural tissue (that is, tissue containing GFAP-positive astrocyte processes). Thus, in all control cases, lesions were judged to be complete transections. Because these were horizontal sections, however, we cannot exclude the possibility of some spared axons in the most ventral part of the spinal cord.

In all rats that received grafts, the lesion site contained graft-derived tissue although some grafts had large central cavities (more on this below). Figs. 2B – E illustrate a graft that closely resembles the grafts shown in Lu et al. Here, horizontal sections from near the central core of the spinal cord were immunostained for GFAP (red fluorescence) and for GFP (green fluorescence) to reveal the grafted tissue. The grafts had a different morphology than host spinal cord in that they appeared disorganized and lobulated. Immunostaining for GFAP was higher in the region of the host tissue adjacent to the junction between host and graft, but not as high as in the regions adjacent to the lesion margin in non-grafted controls (compare Figs. 2B with A). It is noteworthy that this and other grafts expanded to form a structure with roughly the same diameter as the normal spinal cord. Also, the grafts adhered to host tissue without interposed cavities or scar tissue, and graft-derived tissue (GFP-

positive) blended extensively with the host tissue of the rostral and caudal stumps so that there was not a distinct boundary between graft and host and the astroglial boundary at the ends of the host tissue was largely obliterated.

Variability in engraftment

The graft illustrated in Fig. 2 closely resembles the grafts shown in Lu et al. There was, however, variability in the extent of engraftment. Fig. 3 illustrates 18 of the 20 cases in the present study; the two rats that received secondary transections are not shown because the transections damaged the grafts. Each panel illustrates a horizontal section taken near the midpoint of the spinal cord. Numbers indicate animal numbers represented in Tables. The 10 grafts shown in panels I–R resemble the grafts shown in Lu et al., in that the grafts fill the lesion site and blend with host tissue rostral and caudal to the lesion. In contrast, the 8 grafts shown in A–H have internal cavities of varying sizes and/or fail to completely fill in the lesion site. It is noteworthy that all of the animals shown in panels I–R were transplanted by Method 2, whereas the rats shown in panels A–H were transplanted by Method 1, which involved removal of scar tissue and implantation of a preformed fibrin/thrombin gel.

There was no obvious relationship between extent of engraftment and the time after cell isolation (Table 3). For example, grafts in rat #25 and 26 filled the lesion site, although #25 received its graft 1.7 h after cell isolation whereas #26 received its graft late in the day 6.4 h post-isolation.

The extent of integration of grafts with host

We use the term “integration” to refer to the extent to which the graft grows to closely appose and intermingle with the host tissue at the rostral and caudal stumps so that there is no sharp boundary between graft and host. Figs. 2B–C illustrates a graft that is well-integrated with host tissue on both rostral and caudal sides. In sections immunostained for GFP using DAB as the chromogen (Fig. 3), integration appears even more extensive because of the large number of GFP-positive axons that extend from the grafts. By the above definition, most grafts were well-integrated with host tissue on both rostral and caudal sides, even when there were large cavities in the core of the graft. In two grafts, there was a sharp boundary between graft and host tissue on the caudal end of the graft (#12, Fig. 3G and number 31, Fig. 3Q). Even with the sharply defined margin, however, many GFP-positive axons extend from the graft (more on this below).

The presence of partitions within the grafts

An unexpected finding was that most grafts had a single transverse partition in the core of the graft, often near the middle of the graft (Figs. 2B&C, white arrow). Immunostaining for GFAP was high on both sides of the partition (Figs. 2D & E). Partitions of this sort were not reported by Lu et al. In the graft shown in Figs. 2D&E, there was no separation between the GFAP-rich zones on each side of the partition, and there appeared to be some intermixing of glial processes across the partition. In 4 other rats, the grafts resembled the one shown in Figs. 2B – E (see Table 6) in that there was a transverse partition within the graft, but there was not a large separation at the partition. In other cases, however, the partitions were wider and contained non-neuronal scar tissue, creating greater separation between rostral and

caudal portions of the grafts (Figs. 4A&B). No GFAP-positive processes extended into this non-neural tissue. Assessment of the full series of horizontal sections taken at 180 μm intervals revealed that the partition was present throughout the dorso-ventral extent of the spinal cord. Most partitions were oriented in the transverse plane and were continuous in a more or less straight line from one side of the spinal cord to the other. Partitions with non-neuronal scar tissue were seen in 9 rats (Table 6). The presence of the partitions with non-neural scar tissue invites the speculation that the grafts on each side of the partition grew and differentiated, but that there was no fusion of the rostral and caudal parts of the graft to create a continuous bridge of neural tissue.

In 2 cases (Rat #3 and 18) the partition appeared to be bridged by graft tissue (Figs. 4C&D). Notches indicating a partition can be seen on the edges of the tissue (arrows), but in the central core of the spinal cord, the graft appears to have perforated the partition to form a continuous framework of GFAP-positive neural tissue between rostral and caudal stumps. Other features of this case are that the graft extends further into the caudal than the rostral stump, and the caudal boundary of the graft appears more distinct than the rostral boundary of this graft or the boundaries in other cases (Fig. 4C). Indeed, the caudal end of the graft appears to be somewhat encapsulated by GFAP-positive processes, some of which are oriented parallel to the graft margin. The boundary here appeared quite different, however, from the partitions containing non-neuronal scar tissue such as in the case illustrated in Figs. 4A&B especially because GFAP-positive processes extend across the partition (10×view of the same case).

In 6 cases (Table 4) large cavities were present in the core of the graft (Fig. 3). Rat #3 had a smaller cavity but is not included in this group because of the bridge of neural tissue described above. Figs. 5A&B, illustrate 2 horizontal sections separated by 180 μm near the central core of the spinal cord in rat #9. Here, the graft extends into and integrates with the host tissue of the rostral stump. On the caudal side, however there is a rim of graft-derived tissue with a large cavity. All these grafts also had transverse partitions as described above. The cavity was caudal to the partition in 4 cases (2,9,11, and 13) and rostral to the partition in two cases (1 and 5).

Although there was a large cavity in the case illustrated in Figs. 5A&B there is a small region where the graft perforates the partition (Fig. 5B), similar to what is seen in Figs. 4C&D.

It is a reasonable minimal requirement that functional benefits of a graft (in terms of locomotor function) would depend on the degree to which the graft creates a bridge between rostral and caudal segments. Accordingly, Table 6 summarizes the 4 patterns of engraftment based on this criterion. Category 1 grafts have at least a partial tissue bridge between rostral and caudal segments; Category 2 grafts have a partition with some intermixing of astroglial processes across the partition; Category 3 grafts have a partition containing non-neuronal tissue, and Category 4 grafts have large cavities.

Native GFP fluorescence of grafts

The sections illustrated in Figs. 2–4A–B were immunostained for GFP to reveal the graft, but even without immunostaining, native GFP fluorescence was evident. Fig. 5C illustrates native GFP fluorescence from an unstained section from the same case shown in Fig. 2C imaged for 3.974 s, which is 8×longer than for the immunostained sections in Fig. 2. When the exposure interval was the same as used for immunostained sections (0.496 s), native GFP fluorescence was barely detectable (Fig. 5D). Although native GFP fluorescence was relatively low, it limited our ability to visualize green immunofluorescence of elements within the main body of the graft (more on this below).

Cell types within the grafts

Horizontal sections from representative cases were immunostained with cell type-specific markers. Fig. 6 illustrates pairs of images of sections imaged for native GFP to reveal the transplants (Figs. 6A, C, and E) and the same section imaged for red fluorescence for NeuN, APC IBA1 and GFAP (Figs. 6B, D, F and H respectively). Immunostaining for NeuN (Fig. 6B) revealed small to medium-sized neurons within the transplant with processes resembling dendrites. Immunostaining for APC (a marker for oligodendrocytes) revealed small-medium sized cells within the transplant with the same general morphology as APC-positive cells within the host parenchyma (Fig. 6D). Immunostaining for IBA1 (amarker for microglia) revealed ramified cells with a morphology similar to microglia in the host parenchyma (Fig. 6 F). Immunostaining for GFAP revealed ramified astrocytes with a morphology similar to astrocytes in the host parenchyma (Fig. 6H and see also Fig. 2).

Ectopic cell masses

Another surprising discovery was that ectopic colonies of GFP-positive graft derived cells were present at long distances from the graft in many rats. We reported the presence of colonies elsewhere (Steward et al., 2014), but note their existence here because they complicate interpretation of the origin of graft-derived axons (see below). Ectopic colonies were found in the central canal caudal to the graft, on the surface of the spinal cord, and in the fourth ventricle of the brainstem. In total, ectopic colonies were found in half the rats that received transplants (Steward et al., 2014).

Assessment of axon outgrowth from the grafts

One of the most dramatic findings in the original study by Lu et al. was extraordinarily robust and long-distance outgrowth of axons from the NSC grafts into the host spinal cord. Our results fully confirmed these findings. As noted by Lu et al., GFP labeled axons could be seen most clearly in sections that had been immunostained for GFP using DAB as the chromogen. Fig. 7 illustrates examples from rat #25, which had Category 2 morphology (see Table 6). GFP-labeled axons streamed out of the graft rostrally and caudally (Fig. 7A) extending longitudinally to both the rostral and caudal ends of the 15 mm long block containing the injury site. Some axons extended longitudinally along white matter tracts in a generally straight trajectory, giving off collaterals that entered the gray matter. Axons also extended within the gray matter with a more tortuous course; these had numerous varicosities along their length suggestive of en passant presynaptic boutons. Fig. 7B

illustrates axons in the lateral column and gray matter about 500 μm caudal to the graft (where counts were taken, see below) and Fig. 7C illustrates axons at the caudal end of the block. GFP-positive cells with the morphology of highly ramified astrocytes were also evident in the host spinal cord about 1–2 mm distant from the edge of the graft (Fig. 7A, arrow). Extensive axon outgrowth can be appreciated in the low power images in Fig. 3. Axon outgrowth was extensive from both rostral and caudal ends of the grafts in 8 of 10 of the cases where the grafts filled the injury site (rat #16, 18, 22, 23, 5, 26, 28, and 32, see Fig. 3). In the other 2 cases in this group (#24 and 31), axon outgrowth was extensive from the rostral end of the graft, but not the caudal (note sharp boundary between graft and host on the caudal end). Even in the cases with cavitation (Figs. 3A–H) there was extensive axon outgrowth.

We counted GFP positive axons at a distance of 500 μm in one rat (#25) in the same way described by Lu et al. There were a total of 48,420 axons, which is actually higher than the value of 29,000 reported by Lu et al. It was our impression that other rats had as many or even more GFP-labeled axons extending from the grafts (Fig. 6), but we did not count axons in other cases.

GFP-labeled axons were also evident in cross-sections taken at low cervical and at thoracic levels below the lesion block. In general, axon density decreased with distance from the graft, but there were halos of GFP-positive axons surrounding the ectopic colonies in the central canal (Figs. 7D&F). The presence of ectopic colonies of graft-derived cells makes it difficult to determine with certainty whether axons at a particular site originated from the main body of the graft or from the ectopic colonies. For example, Figs. 7D&E illustrate a halo of axons around the central canal; this rat (#25) had a mass in the central canal seen in horizontal sections. High magnification views (Fig. 7F) indicate that there were also small GFP-positive masses in the central canal at C8. There were also nests of GFP-labeled axons in the lateral ventral horn (Fig. 7E) that appeared to decorate large dendrites. Co-immunostaining for GFP and MAP2 (a dendrite-specific cytoskeletal protein) confirmed the association between GFP-positive axons and dendrites (Fig. 7G). The size and orientation of the dendrites makes it likely that they are from motoneurons. The presence of displaced cell masses makes it impossible to determine whether GFP-labeled axons seen in cervical levels had grown for long distances from the main transplant or derived from the ectopic colonies. Certainly, the halo of axons centered on the central canal (Fig. 7D) likely originate in part from the ectopic cell masses in the central canal.

Assessment of growth of host axons into the grafts

BDA-labeled reticulospinal axons—In rats that received BDA injections into the reticular formation, large numbers of axons were labeled in the lateral and ventral columns rostral to the lesion, with extensive collaterals that extended into the gray matter. Figs. 8A–D illustrate examples of horizontal sections from two rats. Although BDA-labeled axons were numerous rostral to the lesion, few extended past the host–graft boundary; instead, most ended in structures resembling retraction balls near the graft/host interface. A few BDA labeled axons did enter areas occupied by GFP-positive cells, but because the graft/host boundary is indistinct, it was not clear whether these actually entered the body of the

graft or instead only extended into areas of the host spinal cord occupied by graft-derived cells. In any case, the axons that extended into GFP-positive domains formed small terminal arbors (Fig. 8E). Some of the axons that extended into GFP-positive domains originated as collateral branches from near retraction balls (Fig. 8E). The fact that a few reticulospinal axons enter the graft and form terminal arbors confirms the findings of Lu et al., although on balance, it is the lack of extension into the graft that is more striking.

BDA-labeled reticulospinal axons did not enter the ectopic colonies of cells in the central canal at cervical levels (Fig. 8G). Native GFP fluorescence of the colony of transplant-derived cells is shown in the same section in Fig. 8H.

5HT—Sets of horizontal sections from 4 rats (5, 24, 31, 32) were immunostained for 5HT using Alexafluor-488 to generate green fluorescence. Green fluorescent axons were evident in the host spinal cord in the expected distribution for 5HT-containing axons. In addition, some green fluorescent axons could be seen in the main body of the graft. Because of the native GFP fluorescence, however, we could not be certain that these axons originated from the host. No other sets of sections were available from rat #5, 24, 31, and 32 because these rats were used for BDA tracing. Accordingly, sections from 4 other rats (12, 22, 23, 26) were immunostained for 5 HT using Alexafluor-594 to generate red fluorescence. Red fluorescent axons could be seen in the expected distribution of 5HT axons above the injury/graft and were also present in the portion of the host spinal cord that contained graft-derived cells (Figs. 9B&C, arrow). These appeared to stream from the areas containing high numbers of host 5HT axons. Some of the axons that extended into GFP-positive domains formed terminal arbors with varicosities suggesting en passant synapses.

Surprisingly, there were also 5HT positive axons caudal to the graft (Fig. 9D). These were concentrated within about 1 mm of the graft boundary, but a few 5HT positive axons extended for several mm caudal to the graft (Fig. 9D). Initially, we assumed that 5HT positive axons were from the host, but we were surprised to discover large 5HT positive cell bodies within the graft itself, which had a neuronal morphology (Fig. 9E). Red fluorescent cells were present within the graft in all 4 of the rats that were immunostained for 5HT using Alexafluor-594. In addition, green fluorescent cells with similar morphology were also present in the rats that were immunostained for 5HT using Alexafluor-488. 5HT-positive neurons were thus present in the grafts in all 8 rats that were immunostained for 5HT, making it likely that 5HT positive neurons were present in most if not all of the grafts.

The 5HT-positive cells shown in Fig. 9E are rostral to the transverse partition evident in Fig. 9A (this is a category 3 graft), but large 5HT positive cells with neuronal morphology were also present in the part of the graft that is caudal to the partition (not shown). The presence of 5HT positive cells with neuronal morphology in the graft makes it impossible to determine whether the 5HT positive axons that extend past the lesion into caudal segments are from the host or from neurons in the graft. The latter is more likely, however because there were no 5HT-positive axons crossing through the partition. Nevertheless, when we imaged the region caudal to the graft for both 5HT and GFP fluorescence, no double-labeled axons were detected. This means either that the 5HT positive axons actually did arise from the host or that the 5HT axons did not express GFP at sufficiently high levels to be

detectable. Thus, the question of the origin of the 5HT axons caudal to the graft remains open.

Probable stroke in one grafted rat—In our analysis of brains of rats that received NSC transplants, we were surprised to find one rat with a large cerebral infarct. The infarct had a form and distribution consistent with a stroke resulting from occlusion of a major branch of the middle cerebral artery (MCA). BBB scores of this animal (#2) suddenly declined 2 weeks after grafting, which may indicate the time of the stroke. Data from this animal were excluded from the functional analyses.

Functional assessments

BBB analyses of hindlimb locomotor function—In the original study, Lu et al. report that rats that received full transections and no transplants had little hindlimb movement for the duration of the experiment (BBB 0–2), whereas rats with successful NSC grafts showed improved motor function beginning two weeks post graft with continued improvement up to 6 weeks. Average BBB scores at 42 days post transplantation/graft were approximately 1.5 for controls and 6.5 for grafted rats (estimated from graph in Fig. 5 of Lu et al.). These differences were statistically significant by t-tests on the last 4 testing sessions (3, 4, 5 and 6 weeks post-graft). Our Understanding from communications with Dr. Lu was that in their study, rats were excluded post-hoc from the behavioral assessments if histological assessment revealed that grafts did not meet defined criteria (see below), although this was not explicitly reported. Here we present data for all rats, and then subdivide groups based on the features of the grafts.

Average BBB scores over days for all rats are shown in Fig. 10. It was noteworthy that the initial deficit was less than reported by Lu et al. Their average BBB scores at 7 weeks post-lesion in the control group were 1.5 whereas ours were 2.6. The extent of recovery of hindlimb locomotor function was slightly more in our control group than reported by Lu et al. By the end of the testing period, control rats were on average capable of extensive movement of one joint or extensive movement of one joint and slight movement of one other joint. Our transplant group averaged 2.8 on the BBB at 7 weeks post-transplant whereas the average final BBB scores in Lu et al. were 6.5. There were no significant differences between our groups by repeated measures ANOVA ($F = 0.07$, $p = 0.80$), but changes over time were significant ($F = 423.00$, $p < 0.0001$). Fig. 10B illustrates a scatterplot of BBB scores at 5 weeks post transplantation/graft. 6 rats in the transplant group had higher BBB scores in the 6–7 range.

Our understanding was that Lu et al. only included rats in the BBB analyses in which grafts met particular criteria. Our understanding of his communications was that rats were only included “if grafts were adherent to the host over more than 1/3 of their circumference bilaterally”. It was not clear to us how this criterion was applied in practice even after extensive discussions with Dr. Lu. Accordingly, functional data from our experiments were analyzed according to the categories defined above (Fig. 10C); there were no significant differences between groups by repeated measures ANOVA ($F = 0.57$, $p = 0.69$).

Two different surgical techniques were used at the time of grafting; thus, we were curious whether functional outcome differed depending on the method of grafting. To test this, data were analyzed separately for rats that received transplants with and without removal of scar tissue. As illustrated in Fig. 10D, BBB scores did not differ significantly depending on the method of transplantation ($F = 0.25$, $p = 0.79$).

Finally, we asked Dr. Lu to score our grafts using the criteria that he had communicated to us. It was discovered that only 4 of our rats met his inclusion criteria. When BBB scores were analyzed based on Dr. Lu's scoring, there were also no differences between groups (Fig. 10E).

Fig. 10 F illustrates the two rats that were re-transected at 6 weeks post injury. Prior to re-transection, the average BBB was 6, indicating extensive movement of two joints and slight movement of a third. After the re-transection, rats were severely impaired with an average BBB score of 1.25, which indicates slight movement of one or two joints.

Assessment of bladder function—Given the importance of bladder function for people with SCI (Anderson, 2004) we also assessed whether transplant/grafting treatment affected bladder function. A useful measure of bladder function is the amount of retained urine, determined by collecting urine at the time of bladder expression (Fig. 10G). There were no significant differences between groups by repeated measures ANOVA ($F = 0.015$, $p = 0.90$), but changes over time were significant ($F = 6.39$, $p < 0.0001$).

Body weight as an assessment of overall health—Progressive weight gain following SCI is considered to be a sign of good health. All groups gained weight over the course of the experiment ($F = 131.7$, $p < 0.0001$) and there were no significant differences between groups by repeated measures ANOVA ($F = 1.18$, $p = 0.29$).

Discussion

The original report of Lu et al. was remarkable and exciting because of the reported long-distance growth of axons from the graft, ingrowth of host axons, which could form a relay circuit, and five-point improve-menton the BBB scale reflecting recovery of the ability to move all joints of the hindlimbs. Of these 3 key findings, our results confirmed only the long-distance outgrowth of axons from the graft. We did not confirm extensive ingrowth of host axons into the graft or enhanced locomotor recovery in rats that received grafts.

Other aspects of the original report were that freshly isolated NSC's from E14 rats that are treated with growth-factor enriched fibrin matrix expand to completely fill the hole left at the injury site, integrating extensively with host tissue. Our results confirmed these findings. Nevertheless, growth factor treated NSCs are not unique in this regard. Transplants of fetal tissue have been shown to expand to fill lesion cavities and integrate extensively with host tissue (Reier et al., 1986). Also, transplants of either “E14 fetal stem cells” (actually small pieces of freshly-dissected E14 spinal cords), or lineage-restricted neural precursors that were derived by culturing cells from E13.5 rats under defined conditions, can also expand to fill smaller cavities created by partial spinal cord lesions (Lepore and Fischer, 2005).

Our results extend the original study by showing that grafts made using Method 2 completely filled the lesion cavity and blended extensively with the host tissue, whereas grafts made using Method 1 often contained large cavities. Also, most grafts made with either method contained a transverse partition that formed a complete boundary between rostral and caudal ends of the transplants. Taken together, our findings support cautious continuation of development of NSC transplants as a potential therapy for severe SCI, but also reveal that reliable functional benefits remain to be demonstrated and that there are significant barriers to formation of a continuous bridge of neural tissue between rostral and caudal segments. The failure to replicate key aspects of the original report emphasizes the need for cautious interpretation of the impact of findings using this and similar approaches.

Methodological issues

Every attempt was made to duplicate methods used by Lu et al. As is typical with many contemporary journals, their Methods section lacked detail, and so we consulted extensively with the original authors. One of their key concerns was experience with the surgical procedure used and the methods of transplantation; accordingly, we felt that it would be most consistent with the overall goals of the replication project to enlist the aid of the original surgeon to actually do the lesion surgeries and transplantation. The rationale here is the same as for a highly skilled surgical procedure for humans; it is reasonable to have the expert train others in the procedures. Fortunately, the surgeon for the original study (Dr. Paul Lu), was generous enough to do this.

Similarly, we felt that the primary goals of the replication project would be best served to have the original authors prepare the NSC's and growth factor cocktails. This is essentially the same as purchasing a product (drug or biological) from a commercial entity. Fortunately, the original experimental team was generous enough to do this.

Two different methods of transplantation

As discussed in the Methods section, NSC transplants were done in two different ways. In terms of the fidelity of replication, it should be noted that the Methods section in Lu et al. did not specify whether scar tissue was removed at the time of transplantation or not. Our discussions with Dr. Lu revealed that 21 out of 26 of the rats in the original study received transplants using Method 2 and 5 rats received transplants using Method 1 (scar removal with implantation of a preformed fibrin/thrombin gel).

Our results indicate that the best engraftment (large grafts that fill the lesion site) was in rats in which transplants were done without removal of scar tissue (Method 2). In contrast, there were large cavities in the grafts made with scar removal and implantation of a preformed fibrin/thrombin gel. This is actually advantageous from the point of view of therapeutic potential because removal of scar tissue would likely pose a greater risk than transplantation without scar removal.

Grafts made with Method 2 completely filled the lesion site and integrated extensively with host tissue. Extensive integration with accompanying obliteration of the pial/glial scar has been previously reported to occur with fetal grafts (Houle et al., 1999), as well as with transplants of either blocks of fetal spinal cord called “E14 fetal stem cells” (FSCs) or

lineage-restricted neural precursors (Lepore and Fischer, 2005). It should be noted that in the present study, a total of 1.5×10^6 cells were transplanted into large lesion cavities created by complete transections, whereas in Lepore & Fischer, approximately 400,000 cells were transplanted into the smaller lesion cavity created by lateral hemisection injury at C4. Although complete filling of the lesion seems like a good thing, we are not aware of any published evidence that complete filling of a lesion is required for effective anatomical/functional repair.

We can only speculate as to why large cavities form in grafts made with Method 1. One possibility is that the removal of scar tissue creates a second injury leading to inflammatory cell invasion, which could impede the growth of the graft. Alternatively, Method 1 also involves the implantation of a preformed gel of fibrin/thrombin. This preformed gel could create a physical impediment to the growth of the graft. Indeed, the cavities may represent the space previously filled by the gel. Further studies will be required to explore these and other possible explanations.

Lu et al. report that NSCs transplanted without pretreatment with growth factor cocktail did not survive well or grow to fill the lesion cavity. They did not provide data on these control studies, however, and so we did not carry out similar controls in our replication. Based on previous studies (reviewed in Bregman et al., 2002) it would not be surprising that treatment with growth factors was critical for the extensive growth of the grafts in the harsh environment of a complete transection. On the other hand, both E14/FSCs and lineage-restricted neural precursors transplanted without growth factor treatment can expand to fill lesion cavities created by partial hemisections (Lepore and Fischer, 2005).

The presence of a transverse partition in the graft

Some of the grafts in the present study resembled those illustrated in Lu et al. Most did not, however because they had a very distinct transverse partition within the graft. At some of these partitions, there was close apposition of neural tissue of the graft on the two sides (Category 2); at others, the partition was wider and contained non-neural tissue (Category 3). It seems likely that partitions containing non-neuronal tissue would block communication between rostral and caudal segments in category 3 grafts. Clearly, it will be important to further test methods of transplantation to achieve optimal engraftment.

Why transverse partitions develop is unclear. Initially, we speculated that the partitions developed at the site of the original transection. Further consideration, however, indicated that the story is more complex. At the time of the initial spinal cord injury surgery, two cuts were made with scissors about 2 mm apart on one side of the spinal cord and the tissue between the cuts was aspirated. Then the process was repeated on the other side. Thus, there are actually 2 cuts on each side and a large aspirated zone in between. This does not suggest a ready explanation for the development of a single transverse partition. Another puzzling feature is that the partitions are oriented in the transverse plane and continuous in a more or less straight line from one side of the spinal cord to the other. During the initial surgery, cuts were made on one side, tissue was aspirated, and then cuts were made on the opposite side. It would be remarkable if the cuts on the two sides lined up perfectly.

Previous studies have shown that there is substantial dieback of transplanted cells during the first few days followed by expansion, presumably by proliferation (Lepore and Fischer, 2005; Theele et al., 1996). It seems likely that there would have been dieback of cells in the present experiment, although this remains to be documented. One possible explanation is that during expansion, the grafts somehow became anchored to the host tissue of the rostral and caudal stumps early in their growth and the two parts of the graft then expanded independently toward the center of the lesion forcing residual scar tissue to the point at which the two growing ends abutted (thanks to Joseph Bonner for suggesting this possibility). Further assessment of this and other possibilities will require detailed studies of the development of the grafts over time.

Recovery of motor function

There was no statistically significant difference in motor function between grafted and control rats. The lack of motor recovery here vs. in Lu et al. may be due to the fact that most of our grafts had partitions. It should be noted, however, according to our understanding based on communications with Dr. Lu, the functional data presented in Lu et al. came from selected cases in which the grafts were judged to meet specific criteria (see Results).

Long-distance growth of axons from the graft

We observed the same extraordinary growth of graft-derived axons that was described in Lu et al. Tens of thousands of GFP-positive axons crossed the graft/host interface and extended for many mm along the host spinal cord both rostral and caudal to the injury. Again, however, growth factor treated NSCs are not unique in this regard. Lepore and Fischer (2005) show images of alkaline phosphatase (AP)-labeled process streaming from transplants of “E14FSCs”. Interestingly, AP-labeled processes seem less prominent in Lepore & Fischer's images of grafts of lineage-restricted precursors. Although the axonal nature of the AP-labeled processes was not definitively established, the images are similar to what is shown in Lu et al., 2012 and confirmed here. Indeed, the most important advance from earlier studies of axon outgrowth from grafts (Jakeman and Reier, 1991; Reier et al., 1986) is that axons from grafts can now be identified by genetic labeling

5HT-positive neurons in the graft

We were surprised to discover 5HT-positive cells in the graft that appeared to be neurons based on morphology. Also surprising was the presence of 5HT positive axons extending caudally from the graft. We cannot exclude the possibility that the 5HT positive axons caudal to the graft were host axons that regenerated through and beyond the graft, but it is much more likely that they are from the 5HT positive neurons within the graft. Lu et al., saw no extension of 5HT positive axons caudal to the graft and did not comment on the presence of 5HT positive neurons within the graft. The likely explanation is that the dissected embryonic spinal cords in our study included part of the brainstem and 5HT neuron precursors.

Limited growth of host axons into the graft

Tract tracing revealed that some reticulospinal axons were intermingled with GFP-positive tissue from the graft. Intermingling of host axons with graft-derived tissue could reflect either growth of axons into the graft or migration of graft-derived cells into the host. In any case, intermingling of host axons with graft was the exception, and termination at the host/graft boundary was the rule. Thus, although our results confirmed the specific findings of Lu et al., our conclusion is that growth of host axons into the graft was meager. Our results indicate there would be few opportunities to form relay circuits that might mediate recovery of function.

Graft-derived neurons grow robustly across the graft/host interface whereas host axons do not

The fact that graft-derived axons grow past the graft/host boundary readily and extend for many mm whereas host axons largely do not extend into the graft suggests that axons from developing neurons in the graft can overcome inhibitory factors in the terrain whereas host axons cannot.

Conclusion

The present findings confirm robust engraftment of growth factor treated NSCs when implanted into complete spinal cord transection sites leading to complete filling of the cavity, extensive integration with host tissue, and long-distance outgrowth of axons from the graft. Our results did not confirm extensive ingrowth of host axons into the graft or enhanced recovery of locomotor function in grafted rats, no matter how the data were parsed. Our results also reveal differences in engraftment depending on the method of transplantation and reveal that most grafts do not create a continuous tissue bridge between rostral and caudal segments because of the existence of transverse partitions in the graft.

Acknowledgments

Supported by National Institutes of Health NO1-NS-3-2353 and R01 NS047718 to O.S. Special thanks to Dr. Paul Lu for carrying out spinal cord injury surgeries and performing the transplants. Thanks also to Lori Graham for preparing the NSC's for use here, Laine Butler, Jessica Dzubnar, Sabhya Rana, Ardi Gunawan, Jennifer Yonan, and Jamie Mizufuka for assistance in surgical procedures, animal care and testing, data collection and management and neurohistology.

References

Anderson KD. Targeting recovery: priorities of the spinal cord-injured population. J. Neurotrauma. 2004; 21:1371–1383. [PubMed: 15672628]

Basso DM, Beattie MS, Bresnahan JC. A sensitive and reliable locomotor rating scale for open field testing in rats. J. Neurotrauma. 1995; 12:1–21. [PubMed: 7783230]

Bregman BS, Coumans JV, Dai HN, Kuhn PL, Lynskey J, et al. Transplants and neurotrophic factors increase regeneration and recovery of function after spinal cord injury. Prog. Brain Res. 2002; 137:257–273. [PubMed: 12440372]

Buchli AD, Schwab ME. Inhibition of Nogo: a key strategy to increase regeneration, plasticity and functional recovery of the lesioned central nervous system. Ann. Med. 2005; 37:556–567. [PubMed: 16338758]

Busch SA, Silver J. The role of extracellular matrix in CNS regeneration. Curr. Opin. Neurobiol. 2007; 17:120–127. [PubMed: 17223033]

David S, Aguayo AJ. Axonal elongation into peripheral nervous system “bridges” after central nervous system injury in adult rats. Science. 1981; 214:931–933. [PubMed: 6171034]

Filbin MT. Recapitulate development to promote axonal regeneration: good or bad approach? Philos. Trans. R. Soc. Lond. B Biol. Sci. 2006; 361:1565–1574. [PubMed: 16939975]

Fitch MT, Silver J. CNS injury, glial scars, and inflammation: inhibitory extracellular matrices and regeneration failure. Exp. Neurol. 2008; 209:294–301. [PubMed: 17617407]

He Z, Koprivica V. The Nogo signaling pathway for regeneration block. Annu. Rev. Neurosci. 2004; 27:341–368. [PubMed: 15217336]

Houle JD, Morris K, Skinner RD, Garcia-Rill E, Peterson CA. Effects of fetal spinal cord tissue transplants and cycling exercise on the soleus muscle in spinalized rats. Muscle Nerve. 1999; 22:846–856. [PubMed: 10398201]

Houle JD, Tom VJ, Mayes D, Wagoner G, Phillips N, Silver J. Combining an autologous peripheral nervous system “bridge” and matrix modification by chondroitinase allows robust, functional regeneration beyond a hemisection lesion of the adult rat spinal cord. J. Neurosci. 2006; 26:7405–7415. [PubMed: 16837588]

Jakeman LB, Reier PJ. Axonal projections between fetal spinal cord transplants and the adult rat spinal cord: a neuroanatomical tracing study of local interactions. J. Comp. Neurol. 1991; 307:311–334. [PubMed: 1713233]

Jin Y, Fischer I, Tessler A, Houle JD. Transplants of fibroblasts genetically modified to express BDNF promote axonal regeneration from supraspinal neurons following chronic spinal cord injury. Exp. Neurol. 2002; 177:265–275. [PubMed: 12429228]

Jones LL, Oudega M, Bunge MB, Tuszynski MH. Neurotrophic factors, cellular bridges and gene therapy for spinal cord injury. J. Physiol. 2001; 533:83–89. [PubMed: 11351016]

Lepore AC, Fischer I. Lineage-restricted neural precursors survive, migrate, and differentiate following transplantation into the injured adult spinal cord. Exp. Neurol. 2005; 194:230–242. [PubMed: 15899260]

Liu K, Lu Y, Lee JK, Samara R, Willenberg R, Sears-Kraxberger I, Tedeschi A, Park KK, Jin D, Cai B, Xu B, Connolly L, Steward O, Zheng B, He Z. PTEN deletion enhances the regenerative ability of adult corticospinal neurons. Nat Neurosci. 2010; 13:1075–1081. [PubMed: 20694004]

Lu P, Wang Y, Graham L, McHale K, Gao M, Wu D, Brock J, Blesch A, Rosenzweig ES, Havton LA, Zheng B, Conner JM, Marsala M, Tuszynski MH. Longdistance growth and connectivity of neural stem cells after severe spinal cord injury. Cell. 2012; 150:1264–1273. [PubMed: 22980985]

Reier PJ, Bregman BS, Wujek JR. Intraspinal transplantation of embryonic spinal cord tissue in neonatal and adult rats. J. Comp. Neurol. 1986; 247:275–296. [PubMed: 3522658]

Steward O, Popovich PG, Dietrich WD, Kleitman N. Replication and reproducibility in spinal cord injury research. Exp. Neurol. Spec. Issue. 2012; 233:597–605.

Steward O, Sharp KG, Yee KM. Long-distance migration and colonization of transplanted neural stem cells. Cell. 2014; 156:385–387. [PubMed: 24485444]

Theele DP, Schrimsher GW, Reier PJ. Comparison of the growth and fate of fetal spinal iso- and allografts in the adult rat injured spinal cord. Exp. Neurol. 1996; 142:128–143. [PubMed: 8912904]

Tuszynski MH, Steward O. Concepts and methods for the study of axonal regeneration in the CNS. Neuron. 2012; 74:777–791. [PubMed: 22681683]

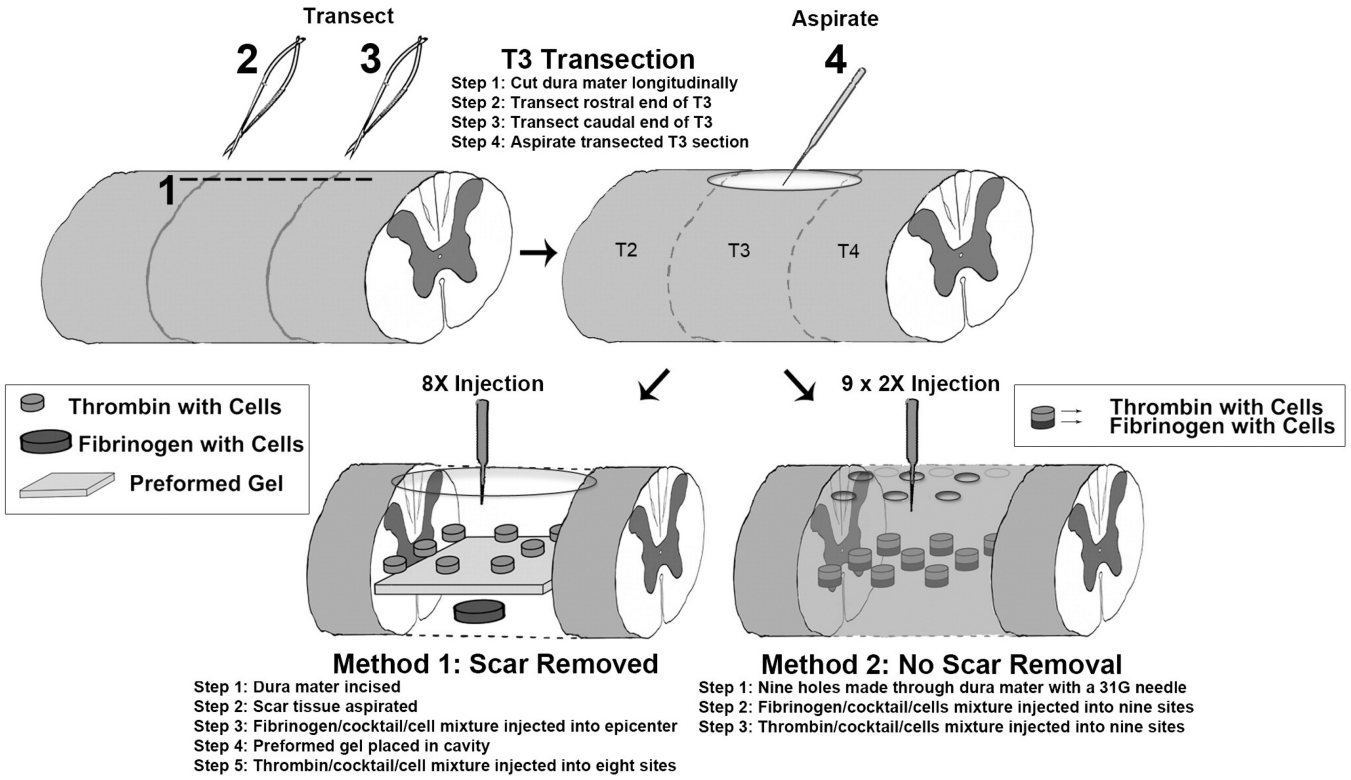

Fig. 1.

Methods of grafting: The diagram illustrates the two methods used for grafting. In Method 1, the dura mater was re-opened and scar tissue was removed prior to injecting NSCs along with a preformed fibrin/thrombin gel. In Method 2, cells were injected through small holes placed in the overlying dura mater without removing scar tissue.

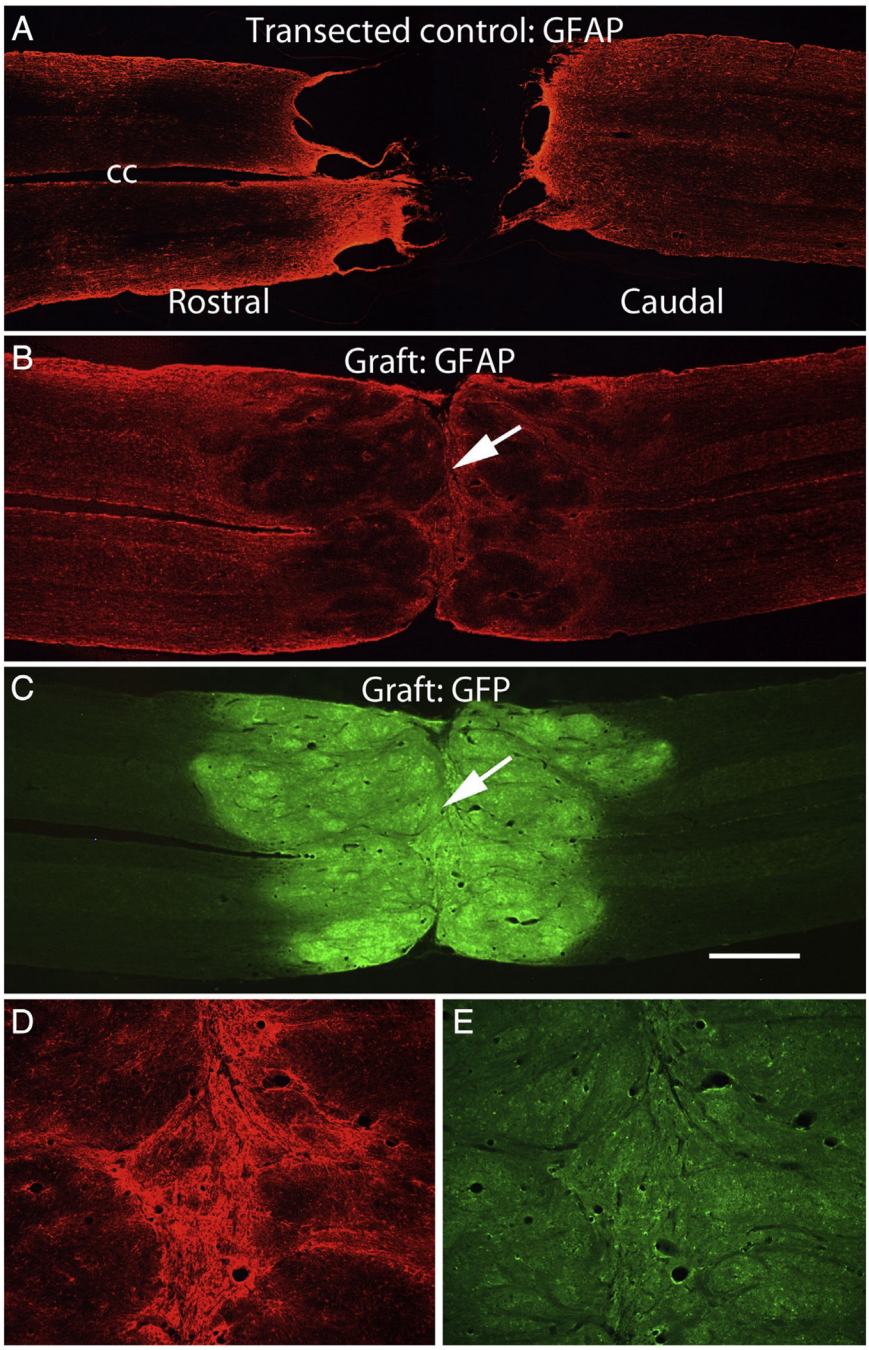

Fig. 2.

Examples of lesion sites in non-grafted control rats and rats that received NSC grafts. A) horizontal section immunostained for GFAP from a non-grafted control. B&C) horizontal section from a grafted rat (#25) co-stained for GFAP (B) and GFP (C). D&E) High magnification views of the partition in the center of the graft in a section immunostained for GFAP (D) and GFP (E). Arrows indicate the partition; cc = central canal. Calibration bar = 1 mm for A–C; 200 μm for D&E.

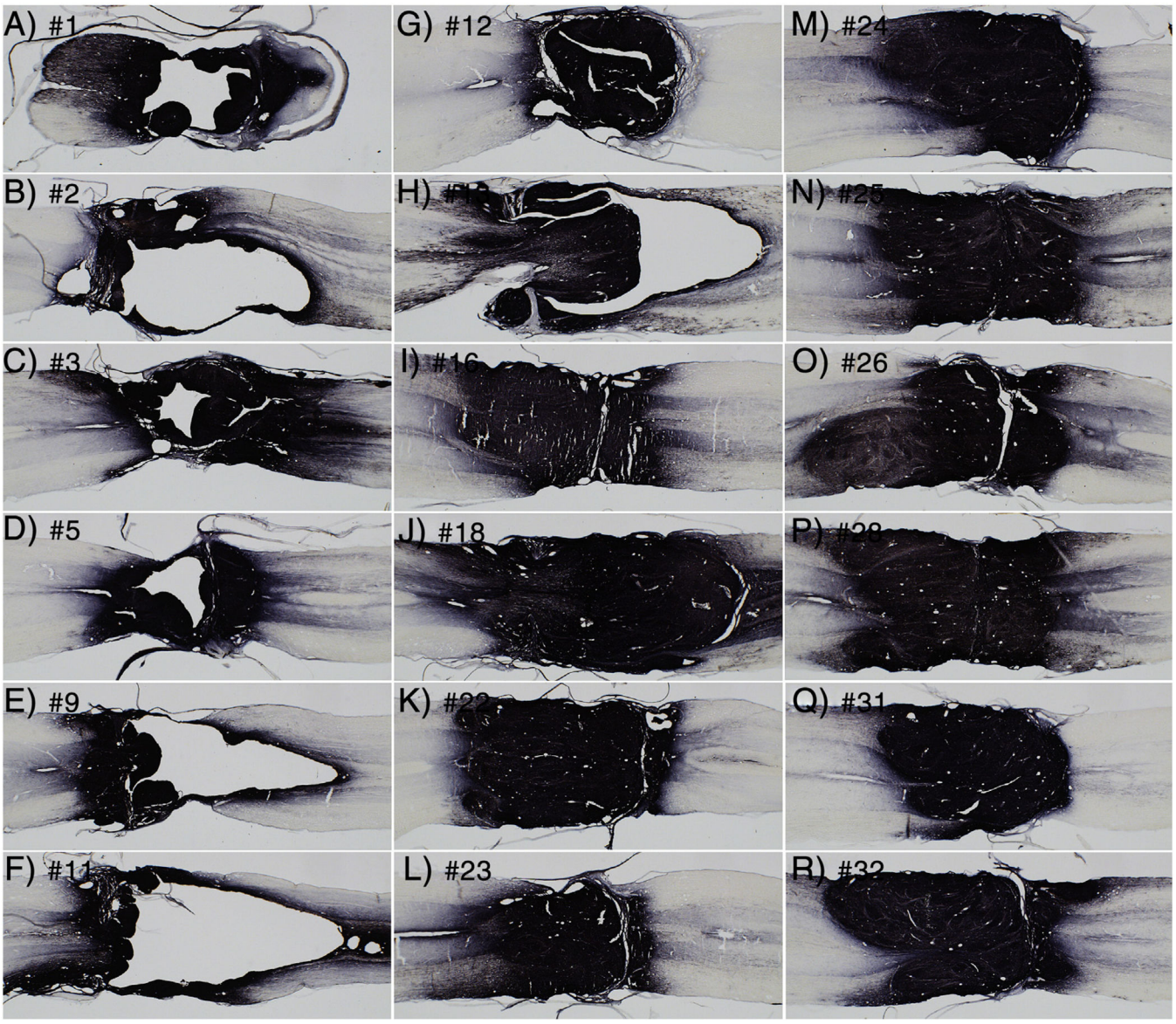

Fig. 3.

Examples of patterns of engraftment. The panels illustrate 18 of the 20 cases in the present study; the two rats that received secondary transections are not shown because the transections damaged the grafts. Each panel illustrates a horizontal section taken near the midpoint of the spinal cord. Numbers indicate animal numbers represented in Tables. The grafts shown in panels A–H were transplanted by Method 1, which involved removal of scar tissue and implantation of a preformed fibrin/thrombin gel. The grafts shown in panels I–R were transplanted by Method 2.

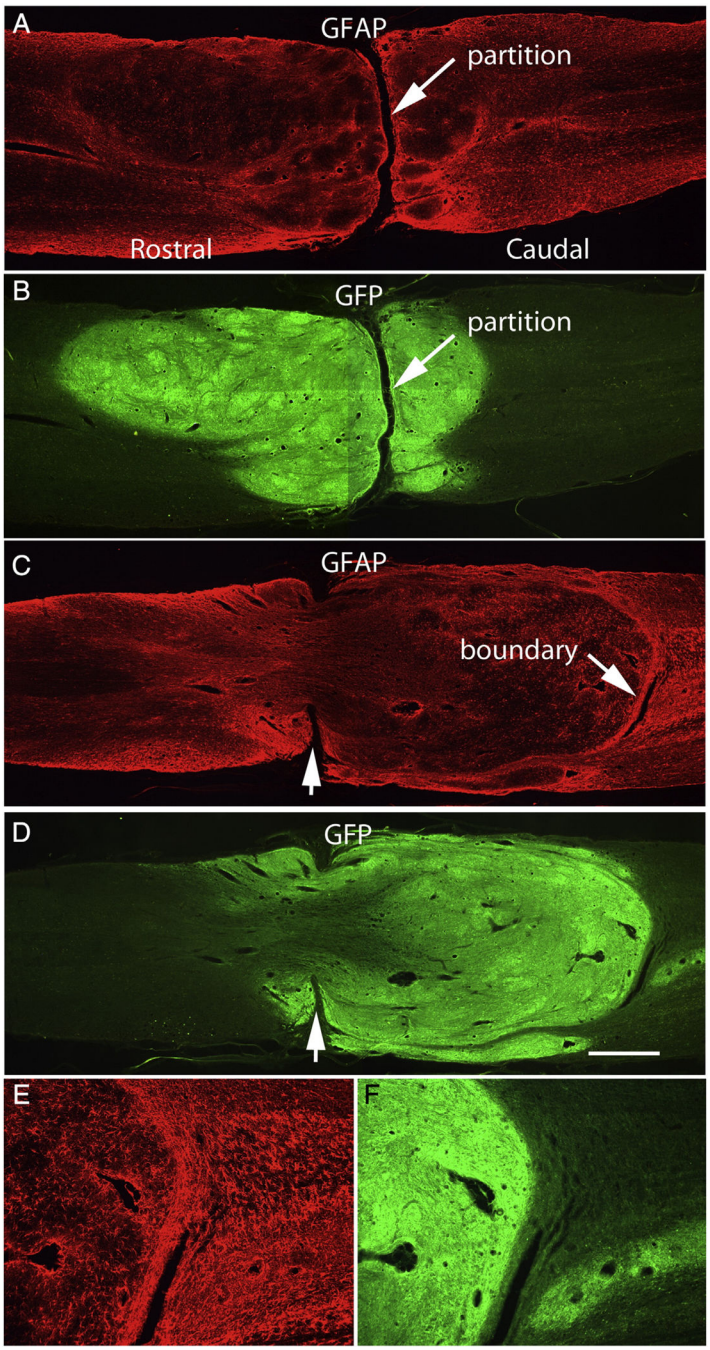

Fig. 4.

Transverse partitions: A&B illustrate a case in which the graft is large and well-integrated with host tissue on both sides but there is a distinct transverse partition separating rostral and caudal portions of the graft. In this case, the partition contains non-neural (scar) tissue. C&D illustrate a case in which the partition is perforated by graft tissue. Notches (arrows) indicate the remaining partition, E&F illustrate the caudal graft/host interface. Calibration bar = 1 mm for A–C; 200 μm for D&E.

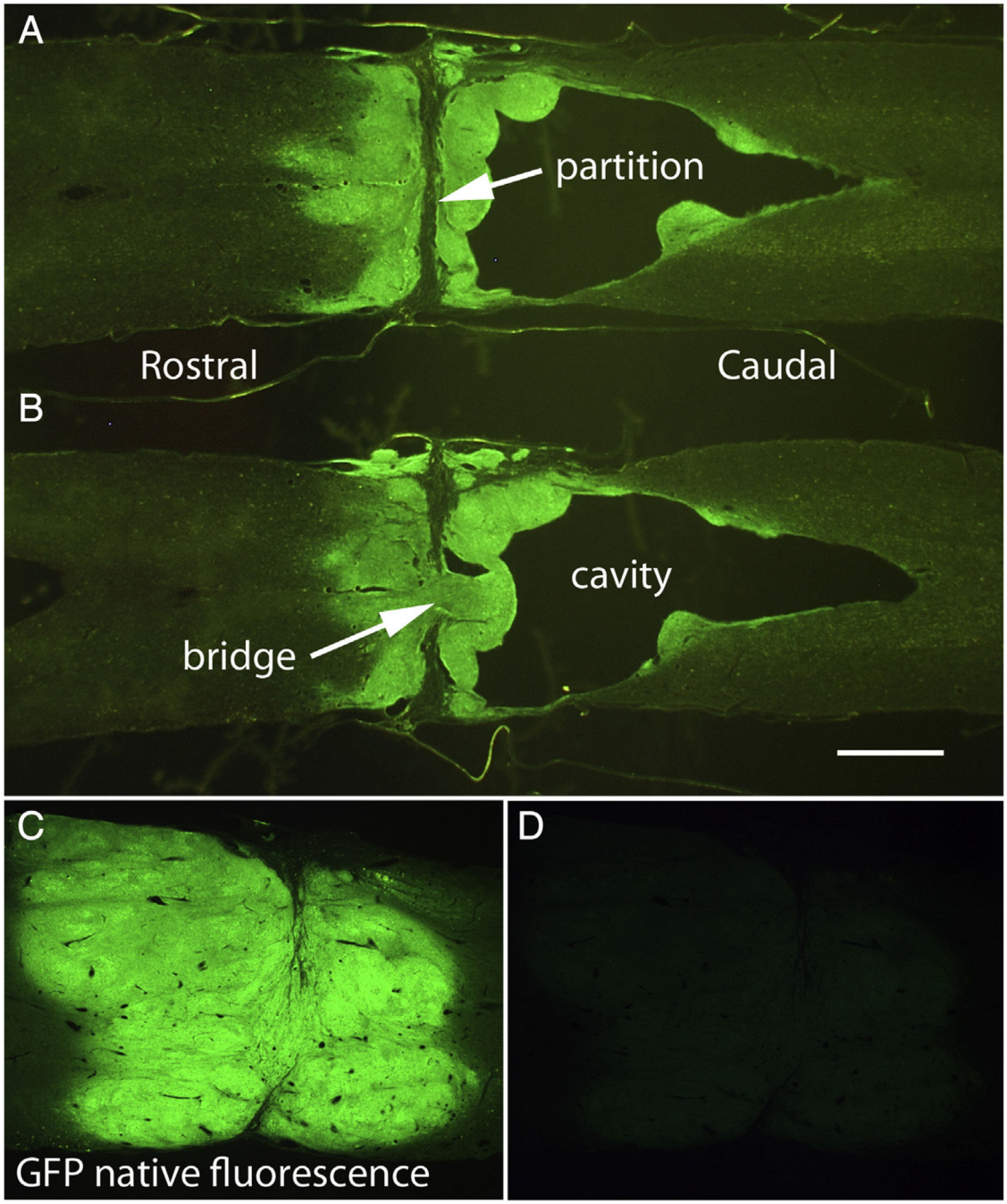

Fig. 5.

Examples of poor engraftment. A&B) 2 horizontal sections separated by 180 μm near the central core of the spinal cord in a case with a large cavity but also some bridging at the transection site. C&D) Native fluorescence of GFP without immunostaining. Exposure time for C = 3.974 s; exposure time for D = 0.496 s (the exposure time used for panels A&B). Calibration bar = 1 mm.

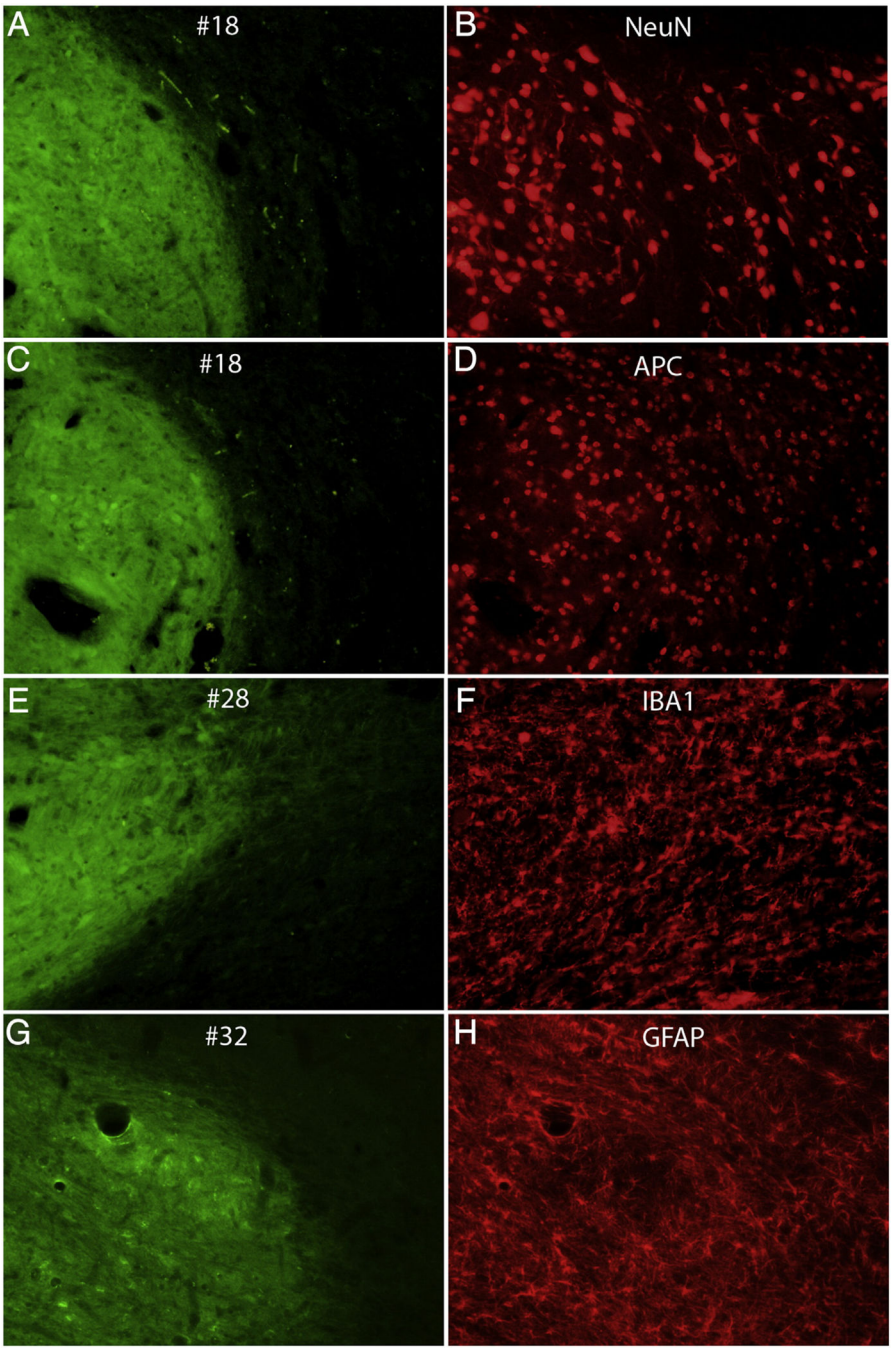

Fig. 6.

Immunostaining with cell type-specific markers. The panels illustrate pairs of images of horizontal sections that were imaged for native GFP to reveal the graft (A,C,E,G) and the same section immunostained for cell type specific markers: B) NeuN; D) APC; F) IBA1; H) GFAP.

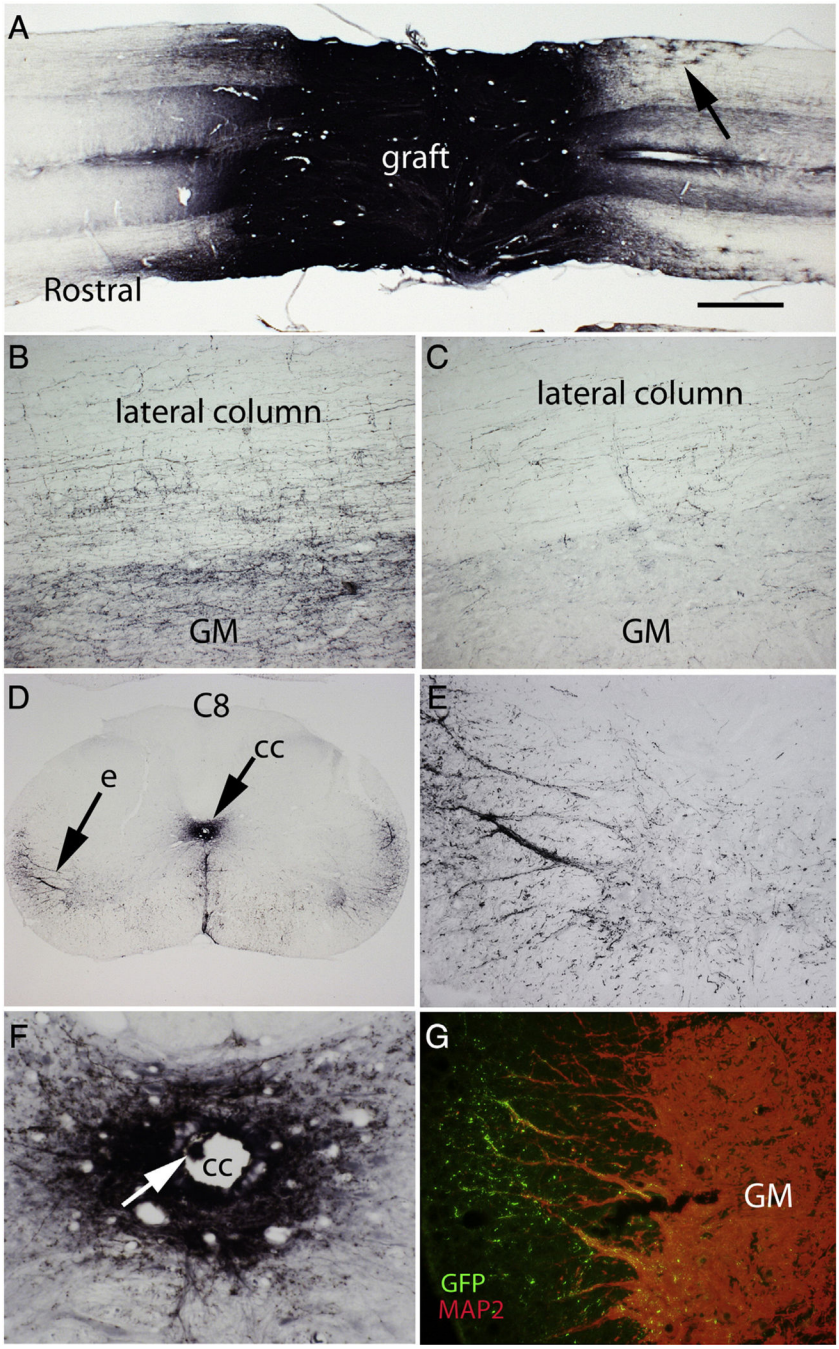

Fig. 7.

Axon outgrowth from the grafts: A) Horizontal section immunostained for GFP to reveal GFP-labeled axons extending longitudinally to both the rostral and caudal ends of the 15 mm long block containing the injury site. This is from Rat #25, which had a category 2 morphology. Arrow indicates highly ramified cells 1–2 mm from the graft with the morphology of astrocytes. B) GFP-positive axons in the lateral column and gray matter about 500 μm caudal to the graft C) GFP-positive axons in the lateral column and gray matter at the caudal end of the block GM = gray matter. D) Halo of GFP-positive axons

surrounding the central canal and nests of GFP-positive axons in the lateral column; “e” indicates the region illustrated at high magnification in panel E. F) Halo of GFP-positive axons surrounding the central canal. G) Region of the lateral column from a section near the one illustrated in E co-stained for GFP (green) and MAP2 (red). Note green GFP-positive varicosities investing the MAP2 positive dendrites that extend into the lateral column. GM = gray matter.

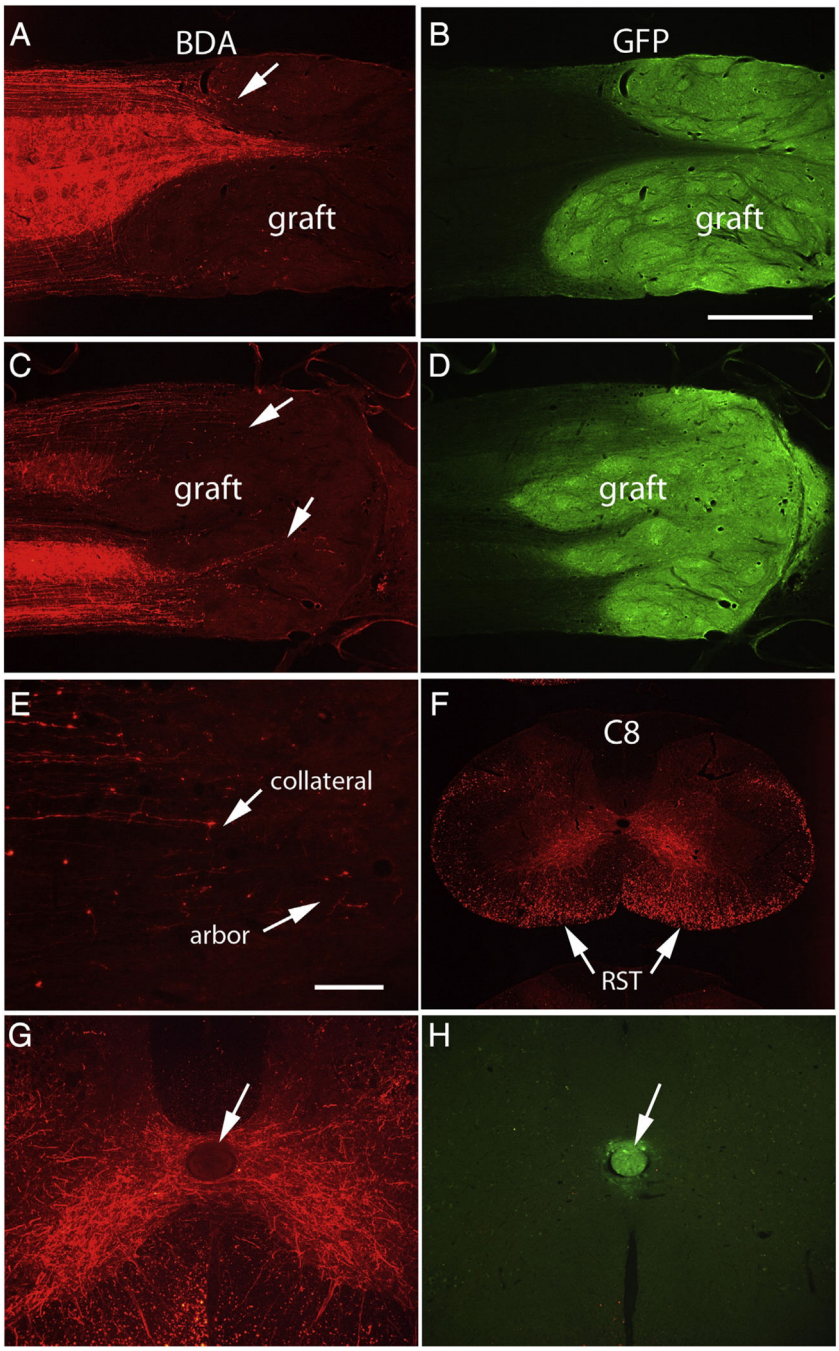

Fig. 8.

Assessment of growth of host axons into the grafts: A) BDA-labeled reticulospinal axons in horizontal section from Rat #32. Most BDA-labeled reticulospinal axons do not extend past the graft/host boundary, although a few do extend into the GFP-positive zone and form terminal arbors (arrow). B) The same section imaged for GFP. C) BDA-labeled axons in a horizontal section from Rat #24. Arrows indicate BDA-labeled axons that enter the GFP-positive zone. D) The section shown in C imaged for GFP. E) Higher magnification view of axons that extend into the graft, some of which originate as collaterals. F) BDA-labeled

reticulospinal axons in a cross-section from C6 from Rat #24. RST = reticulospinal tract. G) BDA-labeled axon arbors criss-crossing the midline in rat #24 at C8 where there is an ectopic graft-derived cell colony in the central canal. Note that labeled axons do not enter the colony (shown by the arrow). The same section imaged for GFP (native fluorescence) to show the graft- graft-derived cell colony in the central canal. Calibration bar in B = 1 mm and applies to A–D and F. Calibration bar in E = 100 μm, and applies to E, G, and H.

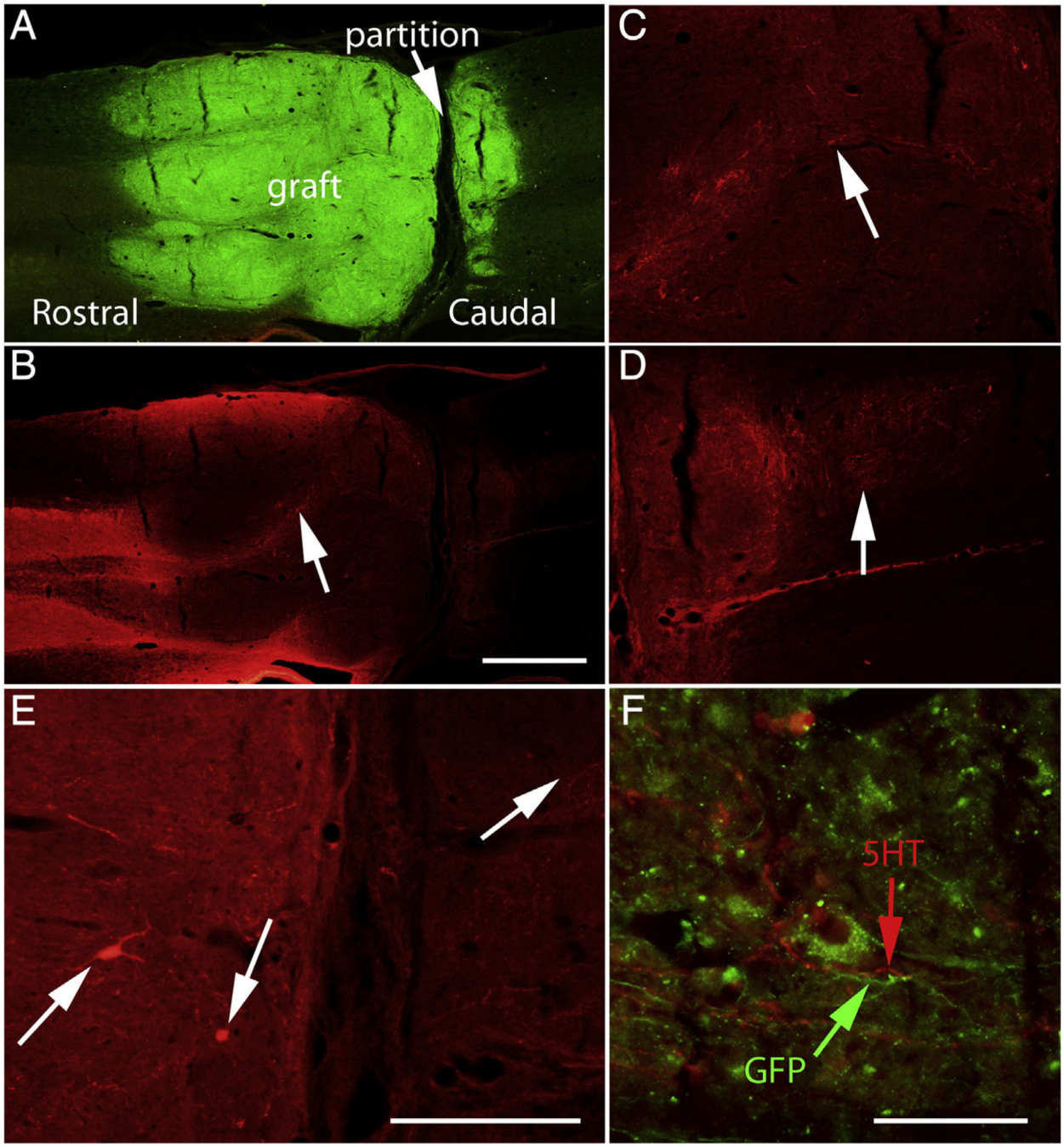

Fig. 9.

Distribution of 5HT-labeled axons: The figure illustrates examples from rat #23, which had Category 2 morphology (see Table 6). A) Horizontal section immunostained for GFP; B) Same section imaged for 5HT. C) Higher magnification view of 5HT-positive axons within the rostral part of the graft. Arrows in B&C indicates 5HT-labeled axons. D) Arrow indicates 5HT-positive axons caudal to the graft. E) Arrows indicate 5HT-positive cells in the graft with neuronal morphology.F) 5HT-positive axons caudal to the graft do not co-

label for GFP. Calibration bar in B = 500 μm and refers to A&B. Calibration bar in D = 250 μm and applies to C and D. Calibration bar in E = 125 μm. Calibration bar in F = 50 μm.

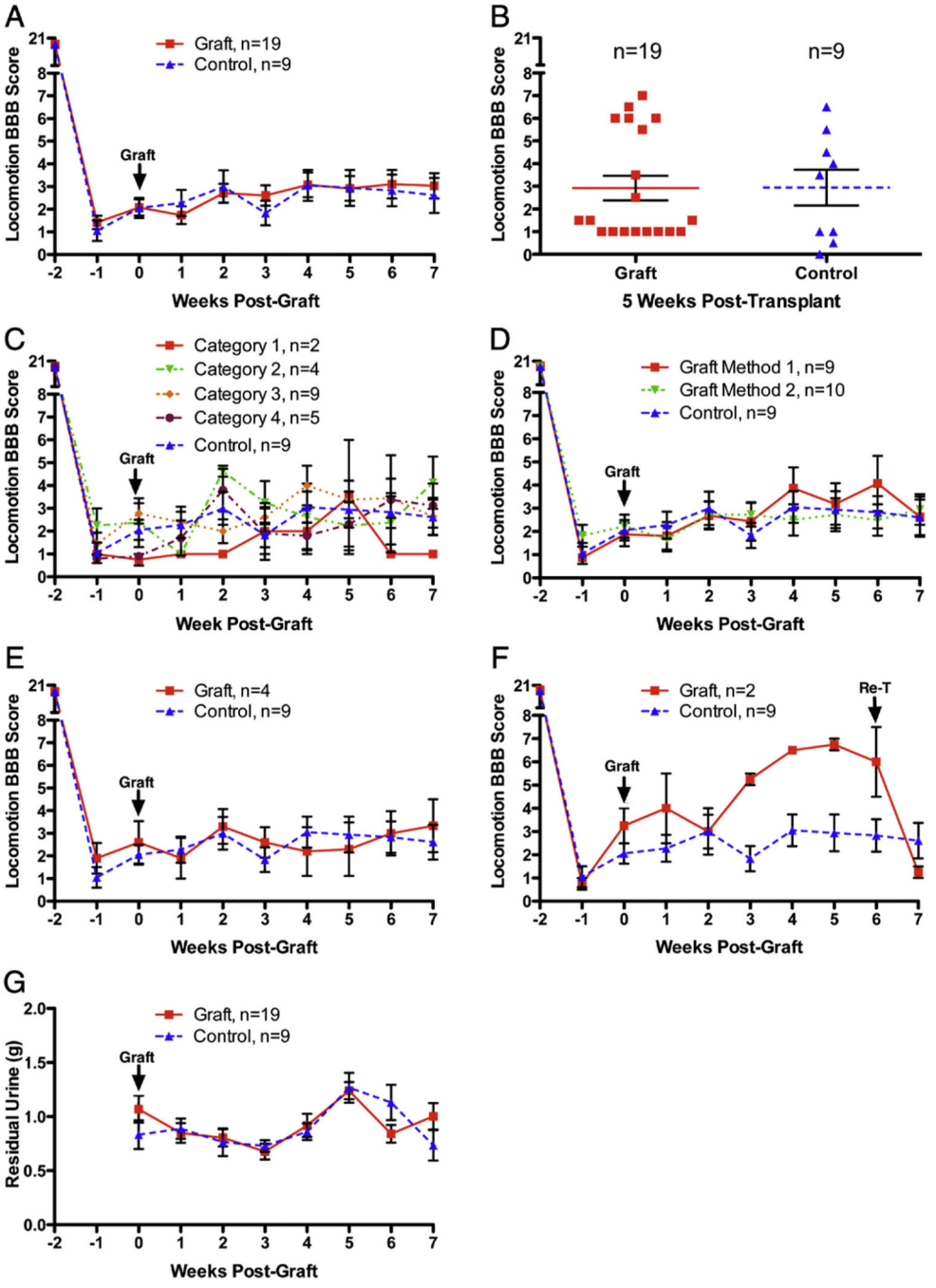

Fig. 10.

Functional assessments: A) Hindlimb locomotor function assessed by the BBB scale for all rats. There were no significant differences between groups by repeated measures ANOVA ($F= 0.07, p = 0.80$); changes over time were significant ($F = 423.00$, $p < 0.0001$). B)Scatterplot of BBB scores at5 weeks post transplantation/graft.C)Comparisonof data from rats with different categories of transplants (as described in Table 6). D) Comparison of data from rats transplanted using Method 1 vs. Method 2. BBB scores did not differ significantly depending on the method of transplantation ($F = 0.29$, $p = 0.79$). E) Comparison of data with

rats selected by Lu as being well-engrafted (n = 4); there were no significant differences between groups by repeated measures ANOVA ($F = 0.57$, $p = 0.69$). F) BBB scores of the 2 rats that received secondary transections vs. controls. G) Plot of volume of residual urine over time. There were no significant differences between groups by repeated measures ANOVA ($F = 0.015$, $p = 0.90$), but changes over time were significant ($F = 6.39$, $p < 0.0001$).

Table 1

Schedule for all surgical procedures.

Squad	T3 transection date	Transplant date	BDA date	Re-transection date
1	4/23/13	5/7/13	6/18/13	6/18/13
2	4/26/13	5/9/13		6/25/13
3	4/30/13	5/14/13	6/28/13	
4	5/2/13	5/16/13	6/28/13	

Table 2

Transplant methods and timing.

Animal #	Date of surgery	Date of transplant	Time after cell preparation (hrs.)	Transplant method (1 or 2)
1	4/23/13	5/7/13	4.2	1
2	4/23/13	5/7/13	7.4	1
3	4/23/13	5/7/13	6.2	1
5	4/23/13	5/7/13	5.3	1
9	4/26/13	5/9/13	5.5	1
10	4/26/13	5/9/13	6.8	1
11	4/26/13	5/9/13	4.3	1
12	4/26/13	5/9/13	3.4	1
13	4/26/13	5/9/13	2.3	1
7	4/23/13	5/7/13	2.4	2
16	4/30/13	5/14/13	4.8	2
18	4/30/13	5/14/13	2.1	2
22	4/30/13	5/14/13	3.7	2
23	4/30/13	5/14/13	5.5	2
24	4/30/13	5/14/13	2.6	2
25	5/2/13	5/16/13	1.7	2
26	5/2/13	5/16/13	6.4	2
28	5/2/13	5/16/13	4.1	2
31	5/2/13	5/16/13	4.6	2
32	5/2/13	5/16/13	5.6	2

Table 3

BDA tract tracing coordinates with an emphasis on reticulospinal tracts.

	Injection	X (M/L)	Y (A/P)	Z (D/V)
Bilateral BDA injections into reticular formation	1	0.8	−11	8.2
	2	0.8	−11.5	8.1
	3	0.8	−12	7.5
	4	0.8	−12.5	7.3

Table 4

Histological methods overview.

Group	Animal #	Histological preparation	Stains	Section sets
Transection only (n = 9)	6, 8, 15, 17, 19, 20, 27, 29, 30	• Horizontal sections through lesion block	• GFAP + Hoescht • Neurofilament + Hoescht	• 1/180 μm sets through lesion for each immunosrain.
Transection + transplant (n = 14)	1, 2, 3, 9, 11, 12, 13, 16, 18, 22, 23, 25, 26, 28	• Horizontal sections through lesion block • Cross-sections at C2, C4, C8, T6, T8, T10, T12, Ll/2 and L4 • Coronal sections through brain	• GFP only • GFP + GFAP + Hoescht • GFP + Neurofilament + Hoescht • 5-HT + Hoescht (rat # 12, 22, 23, 26, 31)	• 1/180 μm sets through lesion for each immunosrain. • Representative cross sections for GFP only.
Transection + transplant + re-transection (n = 2)	7, 10	• Horizontal sections through lesion block • Cross-sections at C2, C4, C8, T6, T8, T10, T12, Ll/2 and L4 • Coronal sections through brain	• GFP only • GFP + GFAP + Hoescht	• 1/180 μm sets through lesion for GFP + GFAP immunosrain. • Representative cross sections for GFP only.
Transection + transplant + BDA (n = 4)	5, 24, 31, 32	• Horizontal sections through lesion block • Cross-sections at C2, C4, C8, T6, T8, T10, T12, Ll/2 and L4 • Coronal sections through brain	• GFP only • GFAP only • GFP + GFAP + Hoescht • GFP + Neurofilament + Hoescht • BDA • GFP + BDA • 5-HT + Hoescht	• 1/180 μm sets through lesion for each immunostain. • Representative cross sections for GFP only and GFP + BDA.

Table 5

Final animal numbers for replication, attrition due to death or removal from study.

Squad	Original numbers	Injury date	Injury type	Died during injury	Died postinjury	Removed from study post-injury	Group	Transplant date	Transplant method	Died posttransplant	BDA date	Re-transection date	Perfusion date	Final numbers	
1	n = 7	4/23/13	T3 transection	n = 0	n = 0	n = 1	Transection only						6/25/13	n = 1	n = 6
							Transection + transplant	5/7/13	(3) Aspiration + 9 pt injection	n = 0			6/25/13	n = 3	
							Transection + transplant + re-transection	5/7/13	(1) 9 pt injection only	n = 0		6/18/13	6/25/13	n = 1	
							Transection + transplant + BDA	5/7/13	(1) Aspiration + 9 pt injection	n = 0	6/18/13		7/9/13	n = 1	
2	n = 7	4/26/13	T3 transection	n = 0	n = 1	n = 0	Transection only						6/28/13	n = 1	n = 6
							Transection + transplant	5/9/13	(4) Aspiration + 9 pt injection	n = 0			6/21/13 6/28/13	n = 1 n = 3	
							Transection + transplant + re-transection	5/9/13	(1) Aspiration + 9 pt injection	n = 0		6/25/13	6/27/13	n = 1	
							Transection + transplant + BDA								
3	n = 10	4/30/13	T3 transection	n = 0	n = 0	n = 1	Transection only						7/2/13	n = 4	n = 9
							Transection + transplant	5/14/13	(4) 9 pt injection only	n = 0			6/28/13	n = 1	
													7/2/13	n = 3	
							Transection + transplant + re-transection								
							Transection + transplant + BDA	5/14/13	(1) 9 pt injection only	n = 0	6/28/13		7/19/13	n = 1	
4	n = 11	5/2/13	T3 transection	n = 0	n = 3	n = 0	Transection only						7/3/13	n = 3	n = 8
							Transection + transplant	5/16/13	(3) 9 pt injection only	n = 0			7/3/13	n = 3	
							Transection + transplant + re-transection								
							Transection + transplant + BDA	5/16/13	(2) 9 pt injection only	n = 0	6/28/13		7/19/13	n = 2	

Table 6

Categorical separation of animals by level of transplant integration.

Category	Animal #	Description of transplant	Transplant method
	6, 8, 15, 17, 19, 20, 27, 29, 30	Transection only	N/A
1	**3**, 18	Graft integrated at rostral and caudal ends with some complete bridging	Method 1 (3) Method 2 (18)
2	16, 24, 25, 28	Graft integrated at rostral and caudal sites, partition present but no or minimal non-neural boundary zone	Method 2
3	**7, 10**, 12, 22, 23, 26, 31, 32	Graft integrated at rostral and caudal sites ; partition present with non-neural zone	Method 1 (10, 12) Method 2 (7, 22, 23, 26, 31, 32)
4	**1, 2, 5, 9, 11, 13**	Extensive cavitation and/or poor integration	Method 1

Bold data represents animals who recieved transplant Method 1.